IN-20

NASA Technical Memorandum 104771

Hypervelocity Impact Testing of the Space Station Utility Distribution System Carrier

Scott Lazaroff

(NASA-TM-104771) HYPERVELOCITY IMPACT TESTING OF THE SPACE STATION UTILITY DISTRIBUTION SYSTEM CARRIER (NASA) 61 p

N93-30507

Unclas

G3/20 0174968

July 1993

NASA

REVISED ERRATA

NASA Technical Memorandum 104771

Hypervelocity Impact Testing of the Space Station Utility Distribution System Carrier

by

Scott Lazaroff

Please disregard earlier errata. Replace pages 13, 15, 17, and 27 with the attached corrected pages.

NASA Technical Memorandum 104771

Hypervelocity Impact Testing of the Space Station Utility Distribution System Carrier

Scott Lazaroff
Lyndon B. Johnson Space Center
Houston, Texas

National Aeronautics and Space Administration
Lyndon B. Johnson Space Center
Houston, Texas

July 1993

Contents

Figures

Figure		Page

Appendix

Tables

Table | Page

Appendix

Acronyms and Abbreviations

Al	aluminum
ATCS	Active Thermal Control System
AWG	American wire gage
cm	centimeter
dB	decibel
ECLSS	Environmental Control and Life Support System
FEP	fluorinated ethylene propylene
GN2	gaseous nitrogen
HAL	Hypervelocity Analysis Laboratory
HIRL	Hypervelocity Impact Research Laboratory
HVI	hypervelocity impact
in.	inches
JSC	Johnson Space Center
km	kilometer
km/s	kilometer per second
kPa	kilopascal
LEO	low Earth orbit
MDA-HB	McDonnell Douglas Aerospace-Huntington Beach
M/OD	meteoroid and orbital debris
µm	micrometer
mA	milliamp
mm	millimeter
MPa	megapascal
NASA	National Aeronautics and Space Administration
OD	outer diameter
PFA	perfluoralkoxy
PIT	pre-integrated truss
PTFE	polytetrafluorethylene
SEM	Scanning Electron Microscope
SRS	Supplemental Reboost System
SSF	Space Station Freedom
t	thickness
UDS	Utility Distribution System
WSTF	White Sands Test Facility

Abstract

The Utility Distribution System (UDS) of the Space Station Freedom (SSF) is, in part, responsible for routing avionic and fluid utilities along the pre-integrated truss segments. These lines are housed in a rectangular aluminum carrier that provides protection from the impacts of meteoroid and orbital debris (M/OD) particles. An initial analysis completed by McDonnell Douglas Aerospace-Huntington Beach estimated that the avionic lines in the UDS carrier could experience approximately 200 failures per year. This number is based on a very conservative failure criteria that any penetration into the avionic portion of the UDS carrier would cause an avionic line to fail. This conservative criteria had to be used because little is known about the effects of M/OD on avionic and fluid lines, especially behind a protective carrier cover. As a result, a two-phase joint NASA Johnson Space Center and McDonnell Douglas Aerospace-Huntington Beach hypervelocity impact (HVI) test program was initiated to develop an improved understanding of how M/OD impacts affect the SSF avionic and fluid lines routed in the UDS carrier.

This report documents the first phase of the test program which covers nonpowered avionic line segment and pressurized fluid line segment HVI testing. From these tests, a better estimation of avionic line failures is approximately 15 failures per year and could very well drop to around 1 or 2 avionic line failures per year (depending upon the results of the second phase testing of the powered avionic line testing at White Sands). For the fluid lines, the initial McDonnell Douglas analysis calculated 1 to 2 line failures over a 30 year period. The data obtained from these tests indicate the number of predicted fluid line failures increased slightly to as many as 3 in the first 10 years and up to 15 for the entire 30 year life of SSF.

Introduction

Since the Space Station Freedom (SSF) will be exposed to a low Earth orbit (LEO) environment (up to a 500-km altitude), it must be designed to withstand both meteoroid and orbital debris (M/OD) collisions. Specifically, the Utility Distribution System (UDS) is required to provide M/OD protection for its fluid and avionic lines to a level that, when considering redundancy and repair capability, provides an acceptable system. Yet, little information exists on how M/OD impacts affect pressurized fluid and avionic lines behind a protective bumper.

For the UDS, the protective bumper is the utility carrier--a rectangular box that runs the length of the Space Station and made of 0.64 mm (0.025 in.) thick 7075-T73 aluminum (Al). There are two primary carriers where utility lines are routed, one on face 2 and one on face 6 of the hexagonal pre-integrated truss (PIT) segments.

One way of estimating the level of M/OD impacts or failures for a particular design is to use penetration equations that have been derived from empirical data of previous hypervelocity impact (HVI) tests. These equations, such as the Cour-Palais or Fish/Summers penetration equations, provide an analytical method to make these estimations. A study performed by McDonnell Douglas Aerospace-Huntington Beach (MDA-HB) in July of 1991 calculated the number of failures that can be expected of the UDS fluid and avionic lines inside the carriers (reference MDA-HB report no. MDC91-H0643, section 4.5.3). The results showed 5650 avionic line failures and 1 to 2 fluid line failures over a 30 year period (or approximately *200* failures/year). *It is important to note that a very conservative failure criteria assumption was used for the avionic lines because of the lack of available data regarding M/OD impacts on utility lines. The assumption used was that any penetration through the carrier would cause an avionic line failure.*

To better understand M/OD impacts and the affect they have on the avionic and fluid lines in the UDS carrier, an HVI test program was initiated. This coordinated test program being performed by the Johnson Space Center (JSC) and MDA-HB is separated into two phases. The first phase of tests, under the direction of the Power Branch of the Propulsion and Power Division, is with segments of inactive avionic lines and pressurized fluid utility lines behind a simulated UDS carrier cover. The second phase uses active avionic lines and pressurized fluid lines (with longer lengths of lines and representative fluid system volumes). These tests in the second phase will be conducted with the articles behind both a simulated UDS carrier and housed in a flight-like UDS carrier.

The testing described in this report covers the HVIs completed on the inactive UDS avionics lines and pressurized fluid lines (phase 1), at the JSC Hypervelocity Impact Research Laboratory (HIRL), from January through May of 1992 and September through October of 1992, respectively. Its primary objective was to perform an engineering characterization of the damage tolerance of the UDS lines inside the carriers. This information will feed directly into building the test matrix for the next phase of the avionic and fluid line tests that is to be conducted at White Sands Test Facility (WSTF). A secondary objective was to investigate the effects of the HVIs on functional characteristics of the avionic lines. Also, a more realistic number of failures of UDS lines inside the carrier will be estimated using the test data and a probability analysis computed by the BUMPER-E M/OD modeling code.

Test Article Description

The test articles used are representative of the UDS avionics and fluid lines which are enclosed inside the carrier in individual sections separated by a thin metal barrier. Figure 1 shows a typical portion of the current baseline configuration of the utility carriers on the PIT.

Avionic Lines

The types of avionic lines tested were secondary power, primary power, coaxial, 1553 data bus, and fiber optic lines. Except for the primary power line tests, the test articles for each HVI were usually two bundles, each consisting of 7 lines that were approximately 30.5 - 35.6 cm (12 - 14 in.) long with minimal spacing between the bundles. The goal here was to provide adequate target area for an accurate shot and enough length of line to capture as much debris as possible. Because interest was being focused on the lines of the bundle that were struck first by the particle/debris, a lot of excess lines in the bundle were not necessary.

The primary power lines had a large enough diameter that bundling was not required, so, two or three individual lines provided a sufficient target area. Figure 2 shows the typical cross sections of the UDS test articles that were used for the HVIs. Some specifications for the avionic lines are given in appendix A.

The test articles were placed approximately 8.5 cm (3.35 in.) behind a 15.2 x 15.2 cm (6 x 6 in.) piece of 0.64 mm (0.025 in.) thick 7075-T73 Al bumper that represented the UDS carrier cover. In an M/OD protection system, the bumper is a single sheet of material that is used to break up the incoming particle. This dissipates the particle's energy and makes the resulting debris cloud less potent. A constant distance of 8.5 cm was used because it represented the worst case (shortest) spacing between the avionic lines and the bumper. According to MDA-HB drawing no. 1F02896 (August 1991), the distance between the UDS carrier cover and the largest bundle had been approximated at 8.5 cm. Furthermore, the size of the bundles could vary and this dimension had not been determined for the actual bundles in the Space Station carrier.

In addition, a witness plate of 0.64 mm thick 7075-T73 Al was placed typically 20.3 cm (8.0 in.) behind the bumper (approximately 11.4 cm or 4.5 in. behind the test articles). This distance corresponds to the depth of the actual Space Station carrier. Information on the dimensions of materials and spacing used for all the avionic tests are also given in tables 1a and 2a.

An example of the typical layout of the avionic test articles and the simulated UDS carrier in the test cell, for a shot with an impact angle of 0° (relative to the projectile's path), is illustrated in figure 3. A photograph of an actual secondary power line test setup, in the JSC HIRL 4.3 mm light gas gun, is shown in figure 4.

Fluid Lines

The tubing used for the fluid line test articles represented the SSF Active Thermal Control System (ATCS), Environmental Control and Life Support System (ECLSS), and the Supplemental Reboost System (SRS). All the tubing was 304L stainless steel and had the following outer diameters (OD) and wall thicknesses:

ATCS: 4.45 cm OD x 0.089 cm wall (1.75 in. OD x 0.035 in. wall); welded
ECLSS: 1.27 cm OD x 0.051 cm wall (0.50 in. OD x 0.020 in. wall); seamless
SRS: 0.95 cm OD x 0.089 cm wall (0.375 in. OD x 0.035 in. wall); seamless

The tubes were cut to about 36 cm (14 in.) lengths and the ends were flared to accommodate 37° military standard fittings. These end fittings were used to adapt the test articles to the 1/4 in. tubing required by the JSC HIRL pressure system. For the large diameter ATCS lines, special reducers had to be constructed by welding a 1/4 in. union to a 1.75 in. plug and drilling a hole through the assembly. These special plugs and the rest of the fluid test article preparations were fabricated at the JSC Thermochemical Test Area.

The spacing between the fluid test articles and the bumper varied depending upon the size of the fluid line being shot. These distances were based on the spacing of the carrier bar from the carrier cover shown in MDA-HB drawing no. 1F02896 and are given in tables 3a, 3b, 4a, and 4b. The bumper and witness plate material (0.64 mm thick 7075-T73 Al) and dimensional specifications used are the same as in the avionic line tests . The witness plate was placed 20.3 cm behind the bumper.

A photograph of one of the ATCS fluid line HVI test setups, at an impact angle of 45° (relative to the path of the projectile), is shown in figure 5.

Test Procedure and System Setup

Avionic Lines

Each avionic HVI test consisted of four parts: a pre-HVI functional check, the HVI shot, a post-HVI functional check, and the visual inspection/physical damage documentation. The functional checks were performed to determine the current carrying capability of the lines before and after the HVI tests. This consisted of light signal degradation measurements for the fiber optic lines, or resistance and dielectric breakdown (current leakage) measurements for the other types of avionic lines. A more detailed description of these functional checks is given in appendix B. Two of the three HIRL light gas guns, the 1.7 mm and the 4.3 mm guns, were used for this portion of the testing. For each shot, the test article was installed at the required impact angle and the target chamber evacuated. The vacuum level in the chamber depended upon which light gas gun was used. The smaller, 1.7 mm (0.07 caliber) gun uses aerodynamic sabot separation, and it was evacuated to approximately 9.5 - 10 torr (about 0.2 psia). The 4.3 mm (0.17 caliber) gun has a rifled barrel and was pumped down to a vacuum level, approximately 0.5 - 2.0 torr (0.01 - 0.04 psia), for the shot. After the shot, the test articles were photographed, examined, and sent through the post-test functional checks. All HVI shots, test parameters, and results of the inspections are discussed in the Test Results section.

Fluid Lines

The testing for each type of tubing was composed of two parts: 1) fluid lines at ambient pressure and 2) fluid lines at maximum on-orbit system pressure. The test article was installed in the target chamber of the 4.3 mm light gas gun at the specified impact angle (figure 5), and the target chamber was evacuated to approximately 0.5 - 2.0 torr (0.01 - 0.04 psia). All of the fluid line tests were performed with the 4.3 mm gun. The test article was then pressurized and the light gas gun was fired. A schematic of the JSC HIRL pressure system is shown in figure 6. After the shot, a visual inspection was made to document the damage on the lines. This included examinations with a borescope, a Scanning Electron Microscope (SEM), and a metallograph. These findings are described in the Test Results section.

Test Results

The main objective of this test program was to gather data on the physical damage to the UDS carrier utility lines sustained from simulated M/OD HVIs. Also, the effects these particles have on the functional characteristics of the avionic lines were examined. The information obtained during the HVI tests and post-shot functional examinations is used to establish a ballistic limit of the utility lines that are protected by the UDS carrier. This leads to a better estimation of the number of avionic and fluid line failures to be expected and a better estimation of whether the current UDS M/OD protection design is adequate.

The term ballistic limit is used to describe the conditions that cause a failure in a particular shield system. For this test program, the shield system consisted of the protective bumper (carrier cover) and the rearwall (fluid or avionic line test articles). A ballistic limit is defined by the parameters of the particle impact such as particle velocity, particle size and material, impact angle, and the type of fluid or avionic line test article. For example, the initial shot at a shield system uses a certain size particle at a set velocity. The particle size is increased (or decreased) until the smallest particle which causes the shield system to fail is found. At that point, a ballistic limit for that system, particle, and velocity has been determined, but for these parameters only. If any one of these variables is changed, then testing must be performed to determine a new ballistic limit.

For this HVI testing, the basic emphasis was to determine what size particle, traveling at approximately 6.5 km/s and hitting the bumper at 0° or 45°, would cause a failure of the avionic and fluid lines in the UDS carrier. In other words, the goal was to establish the ballistic limit of the UDS lines in the carrier for particles striking the cover at 6.5 km/s at an impact angle of 0° or 45°. This data was then directly used by the BUMPER-E impact analysis tool to get a better determination of the effectiveness of the UDS carrier to protect the lines from M/OD (see Conclusions and Recommendations).

A detailed description of the test articles, the shots, and the physical and functional checkout results can be referenced in tables 1a, 1b, 2a, and 2b for the avionic lines and tables 3a, 3b, 4a, and 4b for the fluid lines. A listing of all photographs taken during this test program is given in appendix C.

An important note for this testing is that there are a number of shots where a piece of debris (either from the pump tube piston or a piece of sabot that was shed from around the particle) trailed the particle through the light gas gun and impacted the bumper plate. Based on the visual evidence left by the debris and the expertise of the members of the HIRL, this debris did not affect the damage on the test articles that were sustained from the actual HVI particle. Where there was a question regarding the significance of the debris on the test article damage, a repeat shot was performed.

Avionic Lines

A set of criteria was established for these HVI tests to determine the extent of functional damage the lines would have to receive to classify them as failed. This failure criteria was put together with the help of SSF engineers responsible for the particular type of avionic lines used in these tests. For the power, data bus, and coaxial lines, the failure criteria was > 5 mA of current leakage and/or a 10 - 15% increase in resistance. For the fiber optic lines, a signal loss of 8 - 10 dB constituted a failed line.

Secondary Power Lines

The first set of HVI shots conducted for this test program used secondary power lines as the test articles. Because little was known of the effects of M/OD on avionic lines, the initial shots were conservative using very small particle sizes. Figure 7 shows the bumper and witness plate mounted in the test setup from HIRL shot no. 1941 (post-HVI and with test articles removed). Figure 8 is a close-up picture of these test articles from HIRL shot no. 1941. This shot used a 0.8 mm (1/32 in.) diameter Al sphere traveling 6.66 km/s. The particle penetrated the simulated carrier cover, but did very little physical damage and did not degrade the insulation or increase the resistance of the lines. This is very important because the MDA-HB estimation described earlier used a failure assumption that any penetration through the carrier would cause an avionic line failure. These tests prove that even though the particle penetrates the bumper (simulated carrier cover) a failure does not necessarily result. HIRL shot no. A1492 is another example of the particle perforating the bumper, yet causing no functional deterioration in the lines (figure 9 and tables 1a and 1b).

A precise ballistic limit was not determined for secondary power lines. A 2.4 mm (3/32 in.) diameter Al sphere striking the simulated carrier cover at 45° (HIRL shot no. A1494) was the biggest particle fired at the secondary power lines. It caused a large amount of physical damage (figures 10, 11, and 12), and a few of the test article lines indicated some slight increases in resistance during the post-HVI checkout. There was no dielectric breakdown of the insulation on any of the secondary power lines. For this part of the HVI test program, the parameters of A1494 are on the borderline of the ballistic limit curve, and the WSTF active line testing will better establish this limit.

Primary Power Lines

For the primary power lines, an exact ballistic limit was not identified. The HVI of a 3.2 mm (1/8 in.) diameter Al sphere striking the bumper at 45° (HIRL shot no. A1500) caused significant insulation damage and severed a small number of conductor strands (figures 13 and 14). However, there was no increase in resistance. Dielectric breakdown (current leakage) of the lines was not tested.

Coaxial Lines

The ballistic limit for the coaxial lines is estimated to be near the parameters of HIRL shot no. A1509. For this shot, a 2.4 mm diameter Al sphere striking the bumper at 45° was used, and it damaged one line enough to expose the inner conductor (figure 15). This line did not increase in its resistance reading, but it did have > 5mA of current leakage from the inner conductor to the outer shield. This is enough loss in insulation protection to cause a functional failure of that line (appendix B).

1553 Data Bus Lines

HIRL shot no. A1532 used a 2.4 mm diameter Al sphere striking at 45° and caused significant dielectric breakdown (> 5mA of current leakage = failure assumption) in several lines of both test article bundles. The physical damage to the data bus lines from this shot is depicted in figures 16 and 17. The results of this test indicate that the parameters are well within the ballistic limit since many lines failed. A smaller particle was not shot at these lines, but it will be included as part of the recommendations for the active avionic HVI tests at WSTF.

Fiber Optic Lines

The ballistic limit for the fiber optic lines is found from the HIRL shot no. A1539, in which a 1.6 mm diameter Al sphere impacted the bumper at 45°. The signal losses in the two severely damaged fiber optic lines of shot A1539 were 35.4 and 36.3 dB. Based on the failure criteria, this is significant enough for a functional failure of the line. The physical line degradation associated with shot A1539 can be seen in figures 18 and 19.

The ballistic limit conclusion is reached because a repeat of the A1539 parameters was made (HIRL shot no. A1578), and the post-HVI check showed no loss of light signal through the line. As seen in figure 20, the physical damage is very similar to the damage to the lines from HIRL shot A1539. Thus in a worst case, the parameters of A1539 and A1578 *can* cause a failure in the fiber optic lines and therefore they lie on the border of the ballistic limit curve.

In addition, figures 21 and 22 indicate similar findings described in the secondary power lines summary of results. It can be seen that small particles (< 1.6 mm in diameter) penetrate the bumper, yet cause little physical damage and no functional damage.

Fluid Lines

The failure criteria for this testing must be mentioned before interpreting the results in detail. This criteria is that only *a perforation of the test article tube wall is specifically called a failure* and not a specified degree of spall or depth of an impact crater. These latter two phenomena may have some affect on the strength of the line so that the burst pressure rating of the line is reduced, but for this testing these damage phenomena will not classify the test article as a failed line.

Active Thermal Control System (ATCS) Lines

Several shots were performed with the test articles filled with water and pressurized to 101 kPa (14.7 psia) to simulate liquid ammonia filled lines. The most significant results were obtained from HIRL shot nos. A1622 and A1688. Under the failure criteria stated previously, the ballistic limit parameters found for this testing come from HIRL shot no. A1622. It had a 2.4 mm diameter Al sphere striking the bumper at 45° and approximately 6.5 km/s. The failure criteria for the fluid line tests is a perforation of the tube wall, and this particle caused two perforations, 0.85 x 1.8 mm and 1.52 x 1.52 mm (figure 23). The test article from HIRL shot no. A1688 used a 2.0 mm diameter particle, striking the bumper at 45° and about 6.8 km/s. It sustained some serious crater damage which caused dimpling of the internal wall, but no perforation resulted.

HIRL shot no. A1690 was performed with nearly the same parameters as A1688, except that the water in the line was pressurized to the maximum ATCS pressure of ~ 2.0 MPa (286 psia). This fluid line had serious crater damage which also caused some internal dimpling, but again, no perforation of the wall occurred.

Further structural analyses were performed on the fluid line test articles from shots A1688 and A1690 at the JSC Structures and Mechanics Division Laboratory. Initially, a borescope was used to get a better picture of the internal dimples. Upon identifying some potential detached spall, a series of x-rays was taken to document the tube damage and to determine if any changes in material density had occurred. These radiography pictures were inconclusive.

Next, the lines were cut longitudinally and the internal damage photographed. Figure 24 shows a "rift" in a dimple from the inside wall of the HIRL shot no. A1690 test article. The most heavily damaged area of the lines was subsequently cut from the tubes and the external craters and internal dimples documented using a JEOL JSM-820 SEM. The pieces were then sectioned through the crater location and further documented with the SEM. The SEM examination identified the spalling of the internal tube wall surface, showed the interface between the particle debris and the fluid line, and noted the compression of the grain structure at the point of impact. Figure 25 is an example of a typical SEM photo showing a cross-sectional view of the tube wall from HIRL shot no. A1688, a crater, and the resultant spalling of the inner wall.

In addition, a cross section of the impact area was looked at using a Zeiss AX10MAT metallograph. These metallurgical cross sections further clarified the degree of spalling of the internal fluid line wall . As can be seen in figures 26 and 27, there is significant damage to the test article from HIRL shot nos. A1688 and A1690, respectively.

HIRL shot nos. A1688 and A1690 had some debris from the pump tube piston impact the bumper. This debris may have done some damage to the test articles. The parameters of HIRL shot A1690 were repeated in HIRL shot no. A1800 to make certain the unwanted piston did not cause the damage discussed above. Since A1688 and A1690 used very similar shot parameters, both were not repeated. A1800 was a clean shot and initial inspection showed several dimples on the internal wall of the test article. The fluid line was cut open and these dimples closely compared to the ones found in A1688 and A1690. Therefore, it is concluded (without the need for further destructive analyses) that the damage to the test articles from shots A1688 and A1690 was indeed *caused by the particle* and not some foreign debris.

Based on the criteria that a perforation of the tube wall constitutes a failure, the parameters of HIRL shot no. A1622 are obviously beyond the ballistic limit of these fluid lines. However, the analyses of the test article from shots A1688 and A1690 clearly show major structural damage to the tube wall at that impact point. This results in a weak spot in the line, and may be a concern if a pressure surge were to occur. Nonetheless, it can be concluded that the parameters of HIRL shot nos. A1688 and A1690 are barely below, if not right at, the ballistic limit for these ATCS lines.

Also, HIRL shot nos. A1688 and A1690 were conducted with almost identical parameters except for water pressure. It was determined that the higher internal stored energy of the test article from A1690 did not significantly affect the damage caused during the HVI. The maximum internal system pressure of approximately 2.0 MPa (286 psia) stresses this line less than 20% of its yield strength. The slightly deeper craters and visible internal wall damage on A1690 are more likely due to the lower impact velocity rather than the higher internal pressure.

Environmental Control and Life Support System (ECLSS) Lines

These lines simulated a 1.4 MPa (200 psia) gaseous nitrogen (GN2) ECLSS line that will be used to pressurize the SSF external ATCS tanks and pump module hardware. The first three shots were performed with the test articles at this SSF system pressure (1.4 MPa), and the results indicate that the ballistic limit is near the parameters of HIRL shot no. A1631. In this shot, a 2.0 mm diameter particle impacted the bumper at 45°, and the subsequent cloud of debris created a 0.8 x 0.8 mm and a 1.0 x 1.1 mm perforation in the tube wall (figure 28). HIRL shot no. A1640 used a slightly smaller particle size of 1.8 mm at the exact same parameters and only caused some marring and craters on the external surface of the tube.

Next, the 1.8 and 2.0 mm particles were shot at lines also pressurized with GN2, but only to 101 kPa. The test articles of HIRL shot nos. A1693 (using a 2.0 mm particle) and A1695 (using a 1.8 mm particle) both sustained perforations of the tube wall . Shot A1693 resulted in a hole in the tube approximately 0.6 x 0.7 mm. The penetration in the line from A1695 is 1.1 x 1.6 mm and though it is believed to have been caused by the actual test particle striking the bumper, it could have originated from the piece of debris that followed the particle. This debris impacted the bumper very close to where the test particle did, so it is difficult to determine which may have caused the tube wall perforation. As a result, the parameters of shot A1695 were repeated in HIRL shot no. A1749 and no perforation of the test article resulted. However, two visible dimples on the internal surface were found and on further examination, one of the dimples had detached spall. Therefore, it is determined that the parameters of HIRL shot no. A1693 are just past the ballistic limit for these ECLSS lines, while A1749 (and A1695) is right on the limit.

Supplemental Reboost System (SRS) Lines

Two shots were conducted with lines that represented the SSF SRS lines. The SSF SRS will collect, store, and propulsively dispose of waste gases. For these tests, the lines were pressurized with GN2 to the maximum SRS pressure of 6.9 MPa (1000 psia). No perforations of the tube wall were produced in these two tests, but the test article from HIRL shot no. A1751 did sustain some significant damage (figure 29). There are two particularly large and deep craters that penetrate approximately 0.30 - 0.35 mm into the wall and cause the internal surface of the tube to dimple. These dimples were observed with the borescope, and it appeared that one could have some possible detached spall.

A structural analysis on the line from shot A1751, similar to the one completed on the ATCS lines, was completed and documented. Figure 30 definitely indicates some detached spall on the right internal dimple and the starting of some detached spall on the other (small crack/flaking of material). Further observation under the stereoscopic microscope substantiated the spalling that occurred on the internal surface of the tube. As a result, it is concluded that the parameters from HIRL shot A1751 lie on the borderline of the ballistic limit for these lines.

A slower moving piece of debris (relative to the particle) penetrated the bumper approximately 1.5 cm down and 1.1 cm to the right of the particle impact point. It is similar to the type of debris seen in the ATCS tests. Because of its speed and location and for the reasons discussed earlier for the ATCS lines, it is concluded that the particle and not the debris produced the serious damage to the SRS line described here in the results.

Conclusions and Recommendations

The overall goal of this phase of the HVI test program was to develop an improved understanding of how M/OD impacts affect the SSF avionic and fluid lines routed in the UDS carrier. The need for the program arose from the results of some initial and very conservative analyses which predicted up to 200 failures per year could occur in these UDS lines. This report documents that the program goal was achieved with great success. Specifically, the three objectives of 1) performing an engineering characterization of the damage tolerance of the UDS avionic and fluid lines inside the carrier, 2) investigating the effects of the simulated M/OD impacts on the functional characteristics of the avionic lines, and 3) estimating a more realistic number of failures of UDS lines inside the utility carriers, were sufficiently met. This phase of testing filled a void where little data had previously existed. The information will help demonstrate how good the baseline UDS carrier design is from an M/OD protection standpoint and will feed directly into determining how much extravehicular activity maintenance time is required to replace functionally damaged/failed UDS lines on SSF. A synopsis of the conclusions reached during the testing is given below.

Avionic Lines

First, the JSC HVI tests prove that the conservative assumption used in the initial MDA-HB analysis is not true. This assumption stated that any penetration through the carrier would cause an avionic line failure. Several tests on the secondary power and fiber optic lines show that particles less than 1.6 mm in diameter (which constitute a majority of the particle sizes in the LEO environment) do penetrate the simulated UDS utility carrier cover, but only do minimal physical damage and do not degrade the insulation or increase the resistance of the lines.

In addition, some of the physical damage on the avionic lines seemed severe from a visual standpoint. Insulation was destroyed and often conductors exposed. However, these lines passed the avionic line functional checks, indicating the cabling would work properly. Therefore, they were not considered failures.

These conclusions are made with the understanding that the HVI testing of powered avionic lines at WSTF will add some crucial data that could alter the answers found here.

At the completion of these JSC HVI tests, a vulnerability analysis was performed by the JSC Hypervelocity Analysis Laboratory (HAL) using the BUMPER-E computer model. It predicted the expected number of impacts on the avionics and fluid sections of the UDS carrier for several test particle diameters. A more detailed description of the BUMPER analysis is shown in appendix D. Based on the data obtained from the HVI tests and this BUMPER run (which used an updated environment model and penetration equation compared to the original MDA-HB analysis), a better estimation of the number of failures to the avionic lines was determined. Instead of anticipating up to 200 avionic line failures per year, *approximately 15 failures per year was found to be more realistic.* This number is still conservative and could potentially drop to around *1 or 2 avionic line failures per year*. However, the final determination of the number of avionic line failures will depend upon the outcome of the powered avionic line HVI testing at WSTF.

An additional conclusion reached from the BUMPER-E computer run was that the upper UDS carrier will be hit by more M/OD than the lower carrier. This is due to the type of attitude that the SSF will by flying in LEO. The ratio of impacts on the upper carrier to the impacts on the lower carrier are as great as 10 to 1 when the Space Shuttle Orbiter is docked to SSF. When the Orbiter is not docked, the ratio decreases to about 1.7 to 1.

The data gathered in this testing at JSC also provided a lot of background information for this next phase of tests at WSTF. The following are some recommendations on particle sizes that could be used during those active line tests.

Secondary Power Lines: The initial shot should be with a 2.4 mm or even a 1.6 mm diameter Al sphere striking at 45°. These lines will operate at 120 volts, and under full load conditions they will carry 58 A. Because of the potential of a high current fault, the smaller particle is suggested.

Primary Power Lines: A shot with a 2.4 mm diameter Al sphere striking at 45° should be used as a starting point for a similar reason as described above for the powered secondary power lines.

Coaxial Lines: A shot with a 1.6 mm diameter Al sphere striking at 45° is suggested to be used as a starting point during the active avionic HVI tests at WSTF.

1553 Data Bus Lines: It is recommended that the initial shot should be with a 1.6 mm diameter Al sphere striking at 45°. This is because several lines were found to be functionally damaged with a 2.4 mm diameter particle striking the bumper (HIRL shot no. A1532). A smaller particle might have enough kinetic energy to cause functional damage to a single 1553 data bus line. Thus, the parameters of A1532 could be past the ballistic limit.

Fiber Optic Lines: It is recommended that a shot with either a 1.6 mm or slightly smaller particle (such as a 1 mm) diameter Al sphere striking at 45° should be used as a starting point.

Fluid Lines

An issue with the fluid line tests was whether the internal pressure of the SSF systems would add to the hazard of an M/OD impact. This extra potential energy in the test articles was investigated and found not to be significant for the lines on the Space Station. First, the hoop stress calculated for the fluid lines used in the HVI testing was only 15% to 20% (maximum) of the yield stress of 304L stainless steel. Second, tests conducted on the ATCS and ECLSS lines at system and ambient pressures showed little variance in the degree of damage experienced. For example, the test articles from HIRL shot nos. A1688 and A1690 had very similar amounts of damage on the external and internal wall surface.

Another conclusion was that the initial estimate of 1 to 2 fluid line failures over the 30 year life of the Space Station is slightly low. Based on the distribution of particles calculated by the BUMPER-E run discussed above and the data from the HVI tests, as many as 3 fluid line failures could be experienced in the first 10 years and overall up to 15 for the entire 30 year life of SSF. At the conclusion of the WSTF testing and a more detailed BUMPER-E UDS carrier analysis, a better calculation will be provided.

For the WSTF fluid lines, some slight variations on wall thickness will be used based on additional design information during the planning for phase 2. The data obtained from phase 1 at JSC will help pick the appropriate shot parameters for phase 2, but no recommendations are given at this time.

Acknowledgments

Thanks are extended to all the personnel at the JSC HIRL and HAL who conducted the HVI shots, helped set up the test system, assisted in post-test visual inspection/data analyses, and completed the BUMPER-E computer modeling of the UDS carriers. They include Jeanne Crews, Manager of the HIRL, and Eric Christiansen, Manager of the HAL (both of the Space Science Branch at JSC). Also included are Pat White, Joe Falcon, Jay Laughman, Earl Brownfield, and Lu Borrego (Lockheed support contractors at the HIRL), and Javier Ortega, Jim Hyde, and Gillian Shephard (Lockheed support contractors at the HAL).

Bill Holton, Lockheed support at the Electrical Power Systems (EPS) Laboratory, assembled all the avionic test article cable bundles and performed the pre-HVI and post-HVI checkouts on the power, coaxial, and 1553 data bus lines.

Rick Dean of the JSC Thermochemical Test Area fabricated all the fluid line test articles.

Glenn Morgan, Lockheed support of the JSC Structures and Mechanics Division, performed the SEM and metallograph analyses of the specific fluid lines discussed in the results.

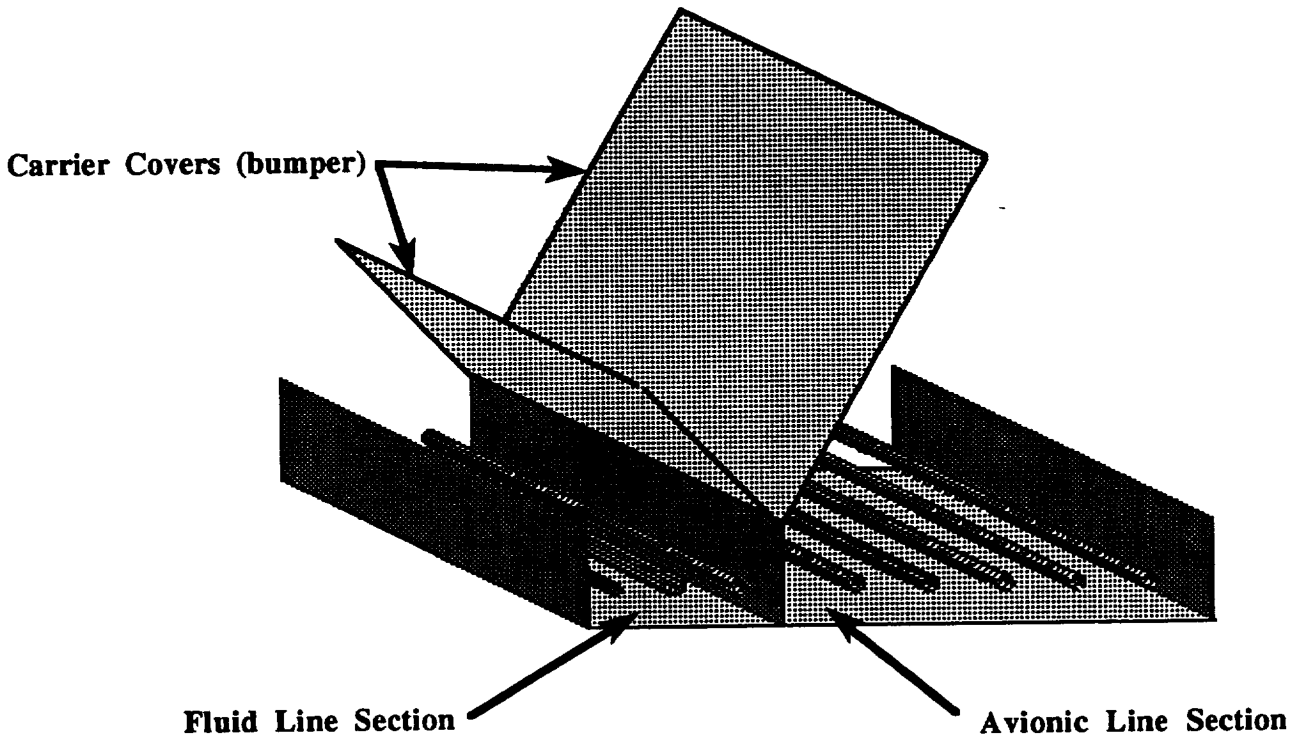

Figure 1. Typical Section of the Baseline Utility Carrier on the PIT

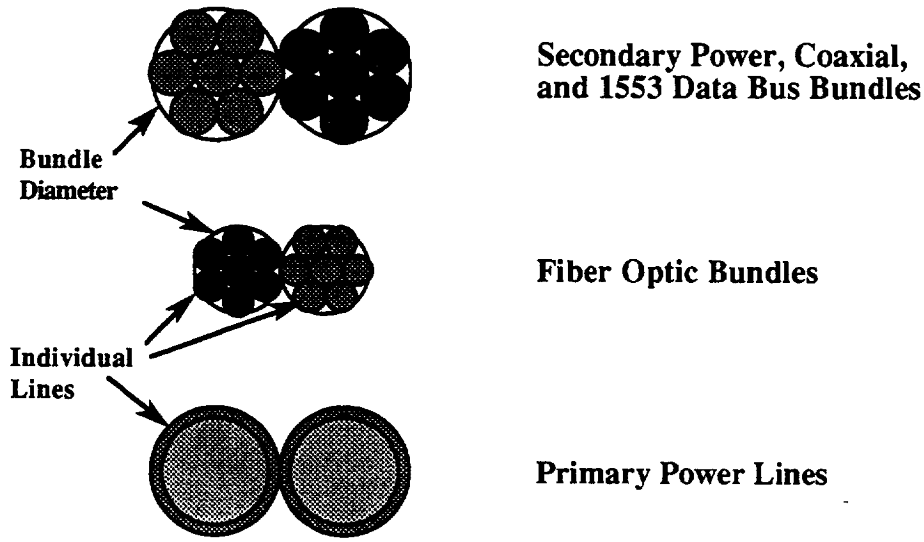

Figure 2. Typical Cross Sections of the UDS Test Articles (not to scale)

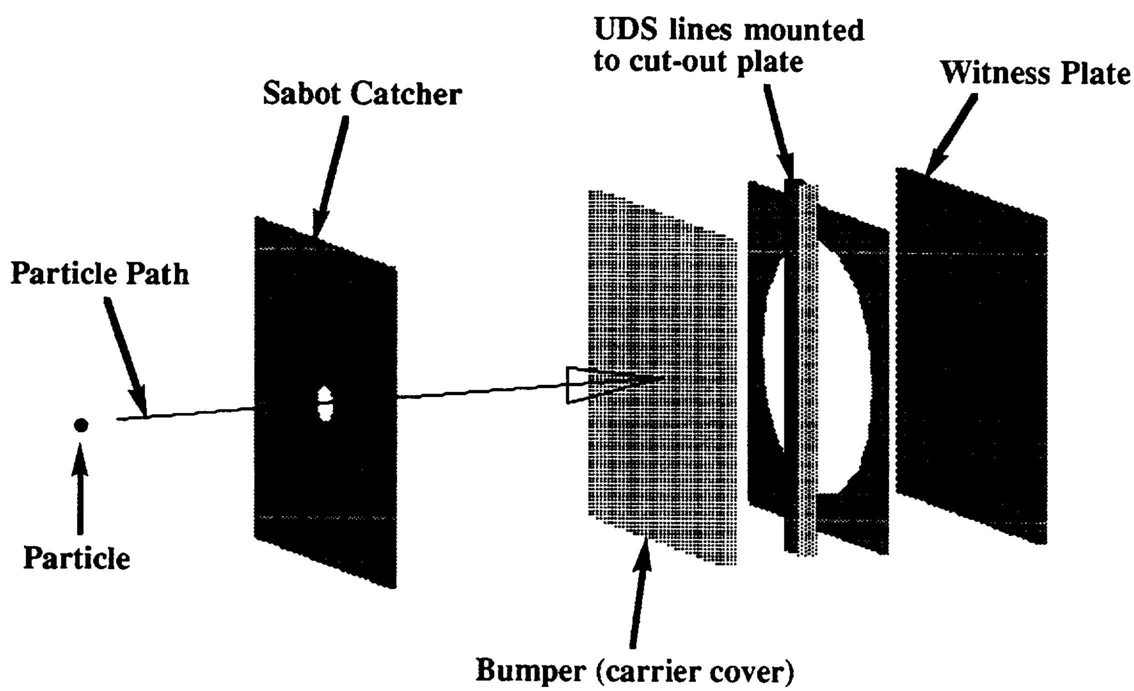

Figure 3. Typical HVI Setup of Avionic Bundle Test Article and Simulated Carrier

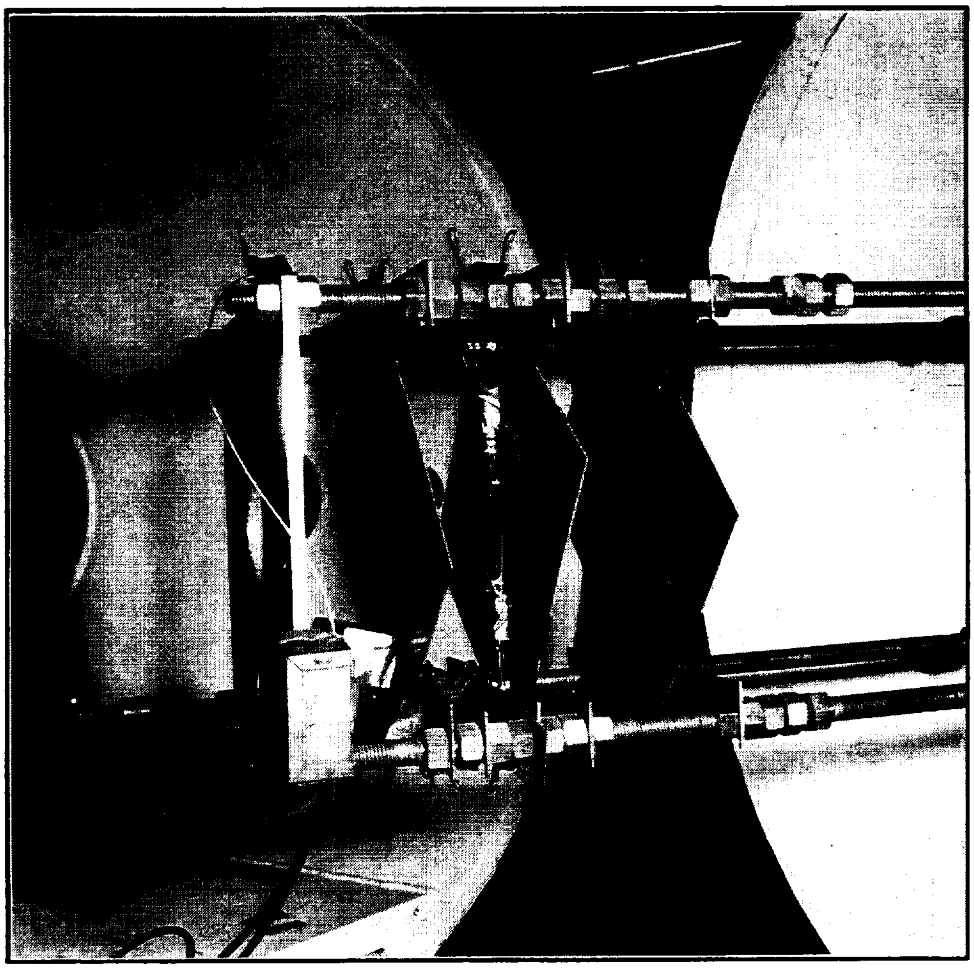

Figure 4. Secondary Power Line Test Setup for a 0° Particle Impact (HIRL Shot No. A1493) in the JSC 4.3 mm Light Gas Gun.

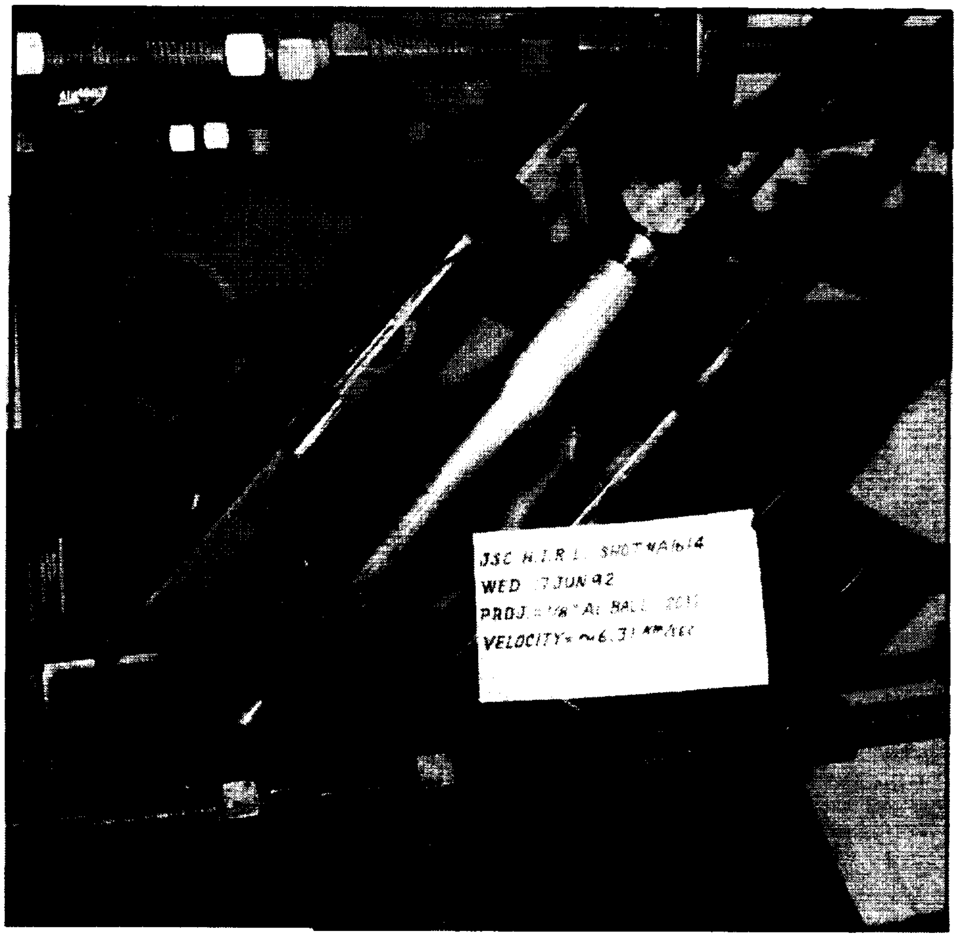

Figure 5. Active Thermal Control System Fluid Line Test Setup for a 45° Particle Impact (HIRL Shot No. A1614) in the JSC 4.3 mm Light Gas Gun

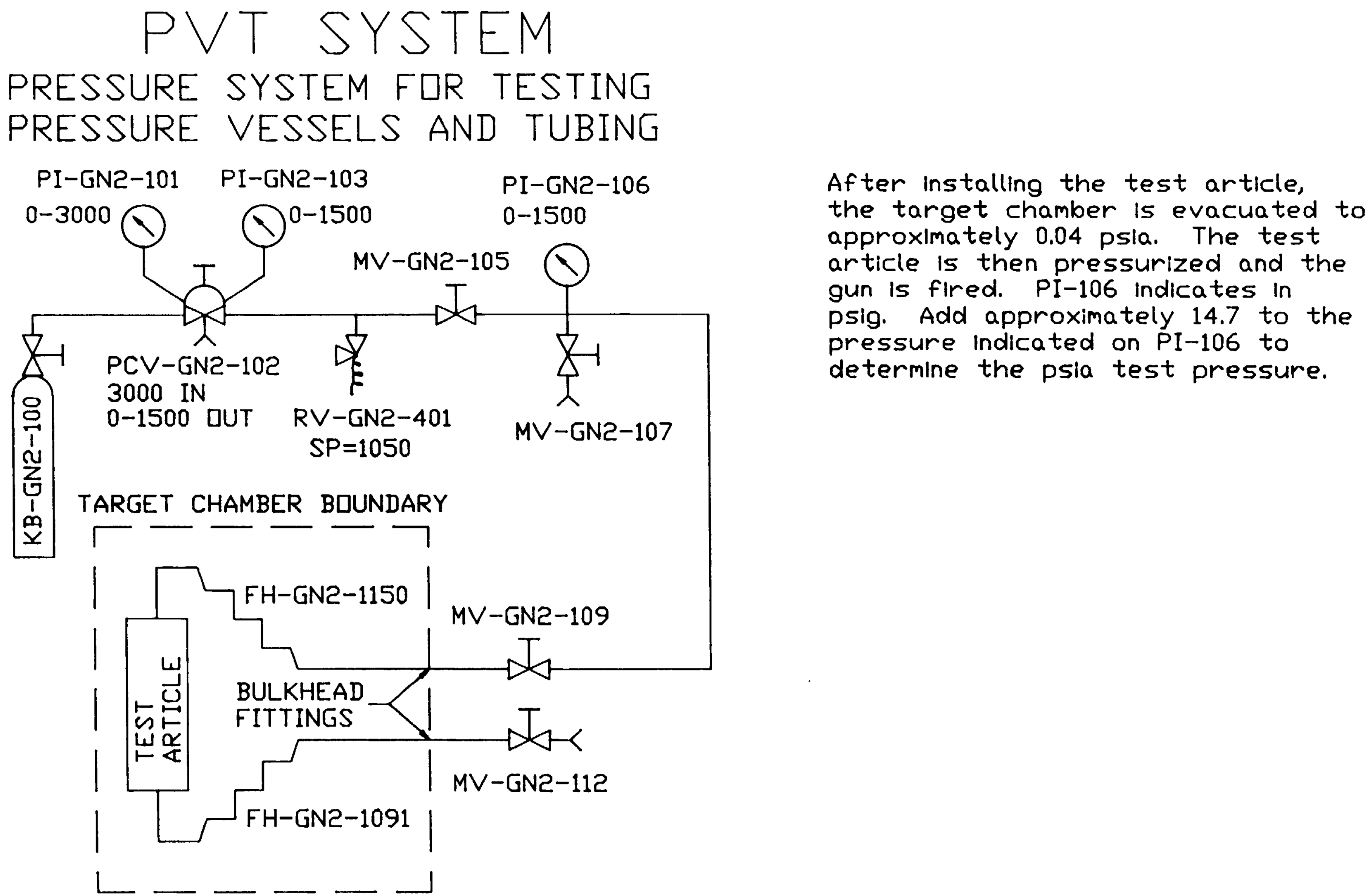

Figure 6. Schematic of JSC HIRL Pressure System

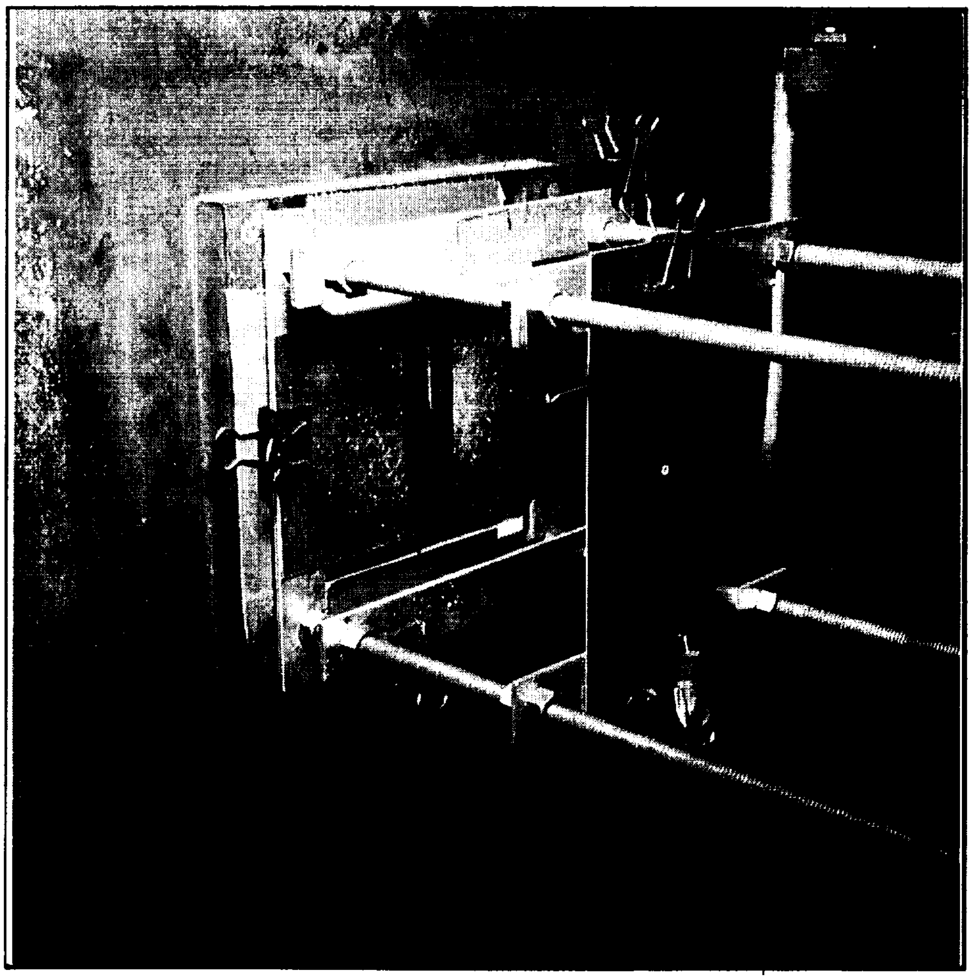

Figure 7. Bumper and Witness Plate Mounted in 1.7 mm Light Gas Gun Test Cell from HIRL Shot No. 1941

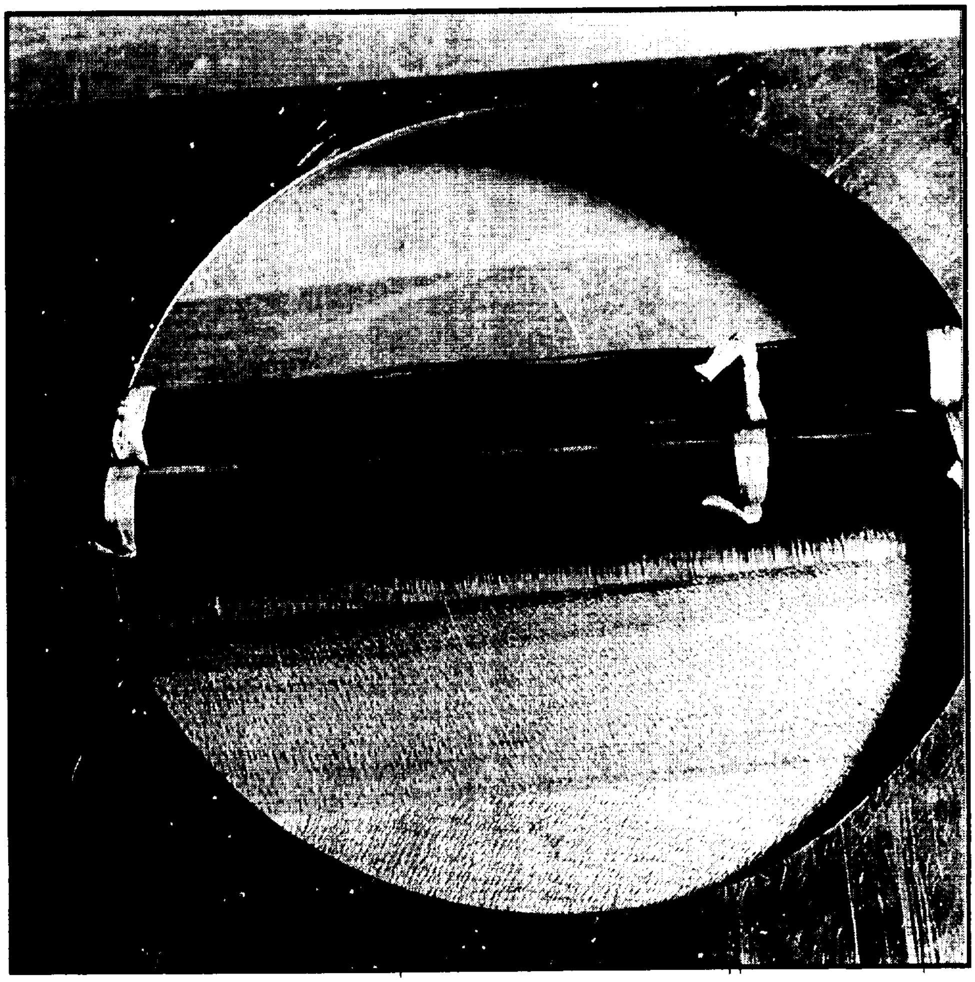

Figure 8. Physical Damage to Secondary Power Lines from HIRL Shot No. 1941

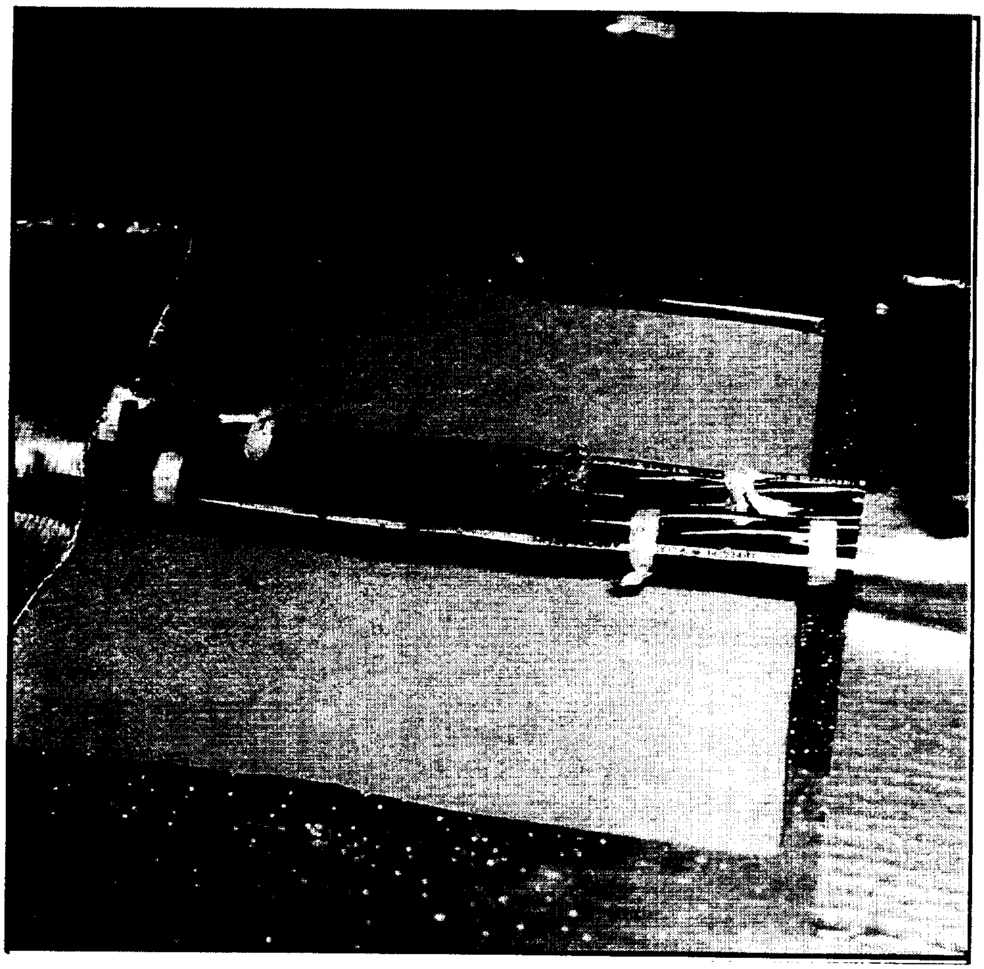

Figure 9. Physical Damage to Secondary Power Lines from HIRL Shot No. A1492

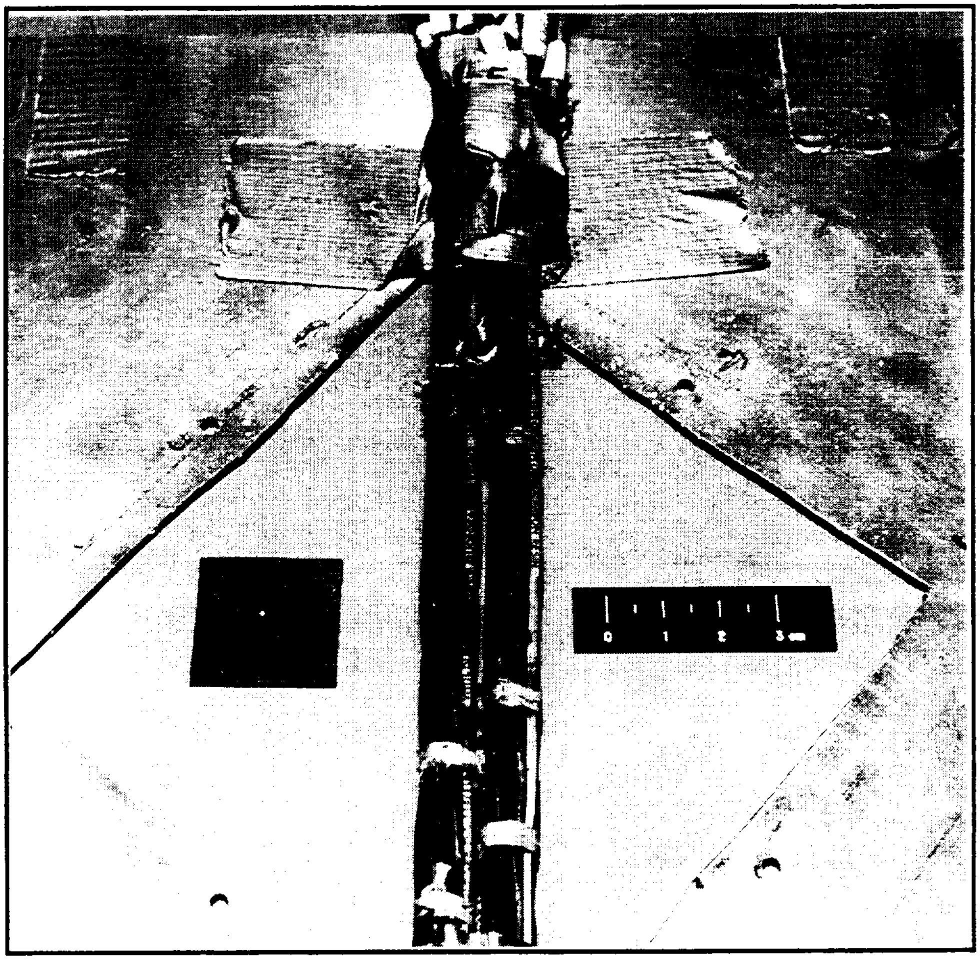

Figure 10. Physical Damage to Secondary Power Lines from HIRL Shot No. A1494

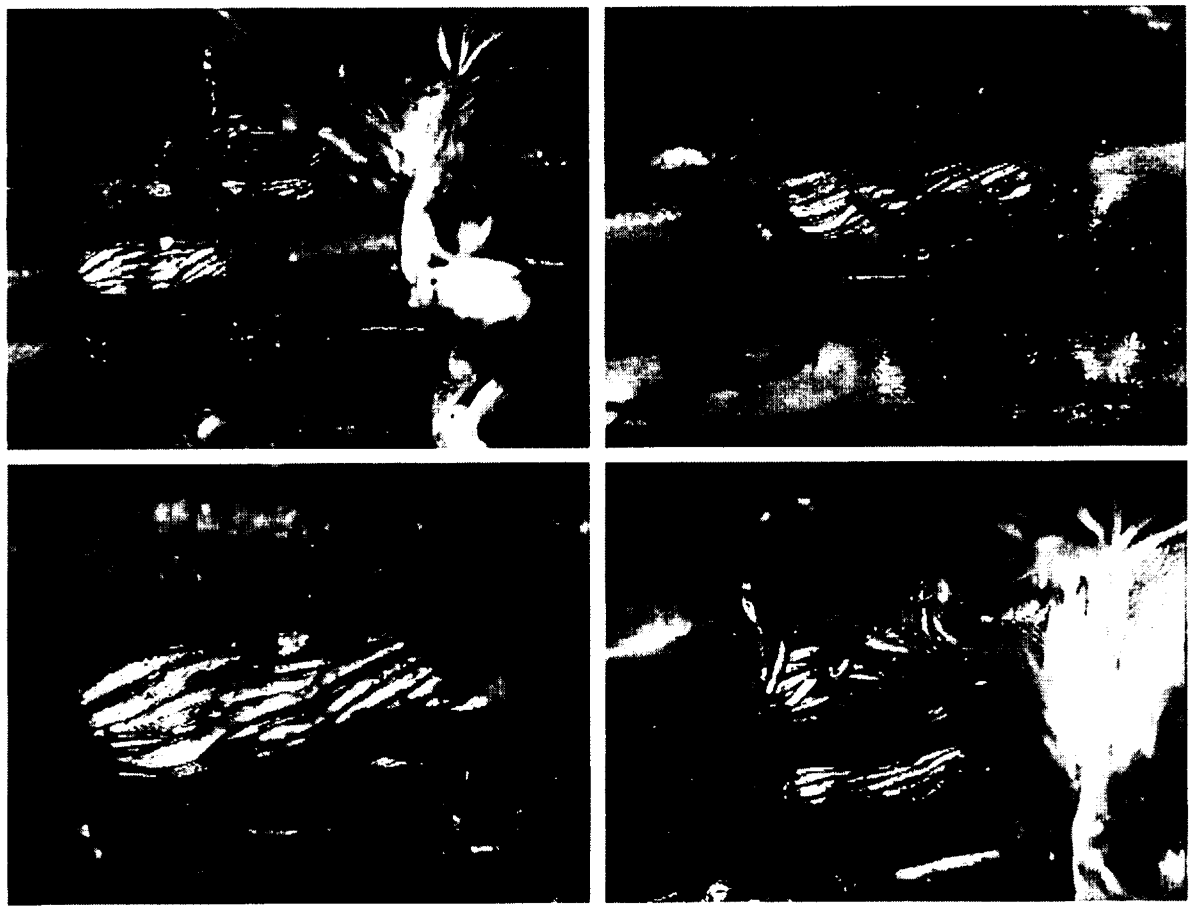

Figure 11. Physical Damage to Secondary Power Line Bundle A2A from HIRL Shot No. A1494 at Magnifications of 10x, 10x, 10x, and 16x (starting upper left, going clockwise)

Figure 12. Physical Damage to Secondary Power Line Bundle A2C from HIRL Shot No. A1494 at Magnifications of 16x, 16x, 10x, and 10x (starting upper left, going clockwise)

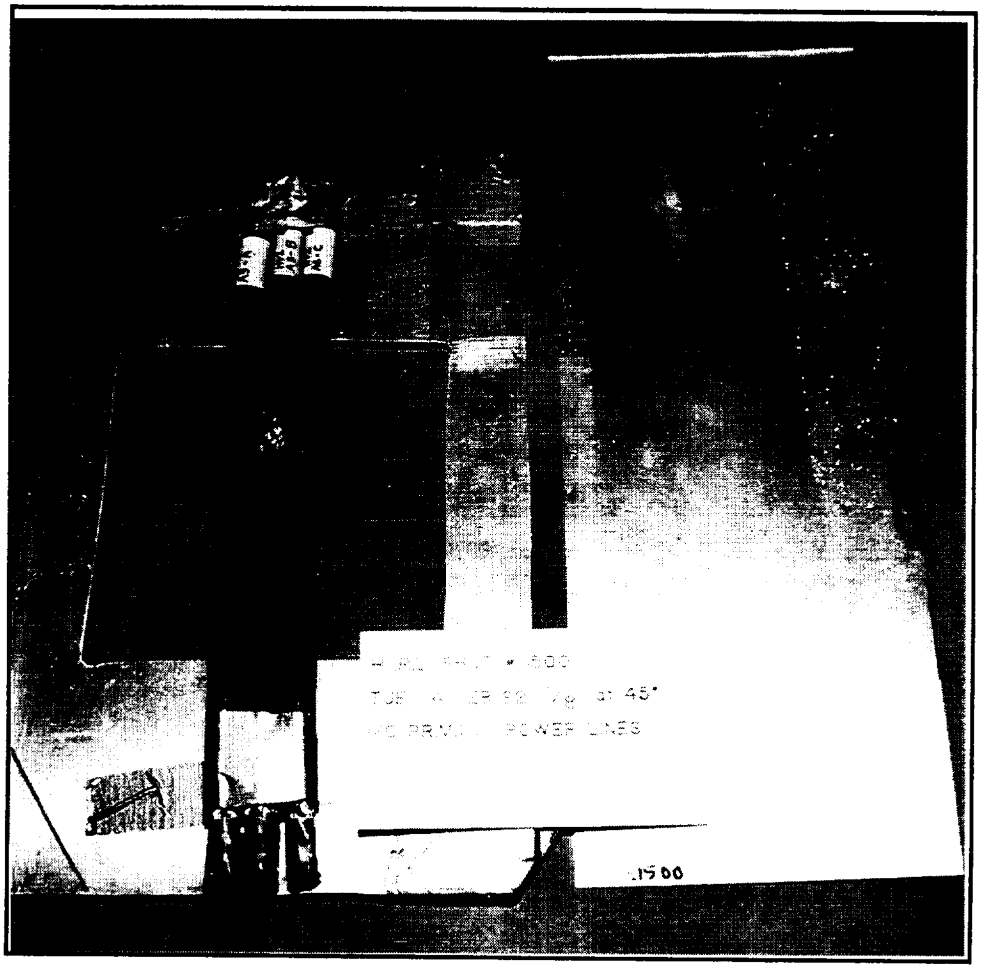

Figure 13. Physical Damage to Primary Power Lines from HIRL Shot No. A1500

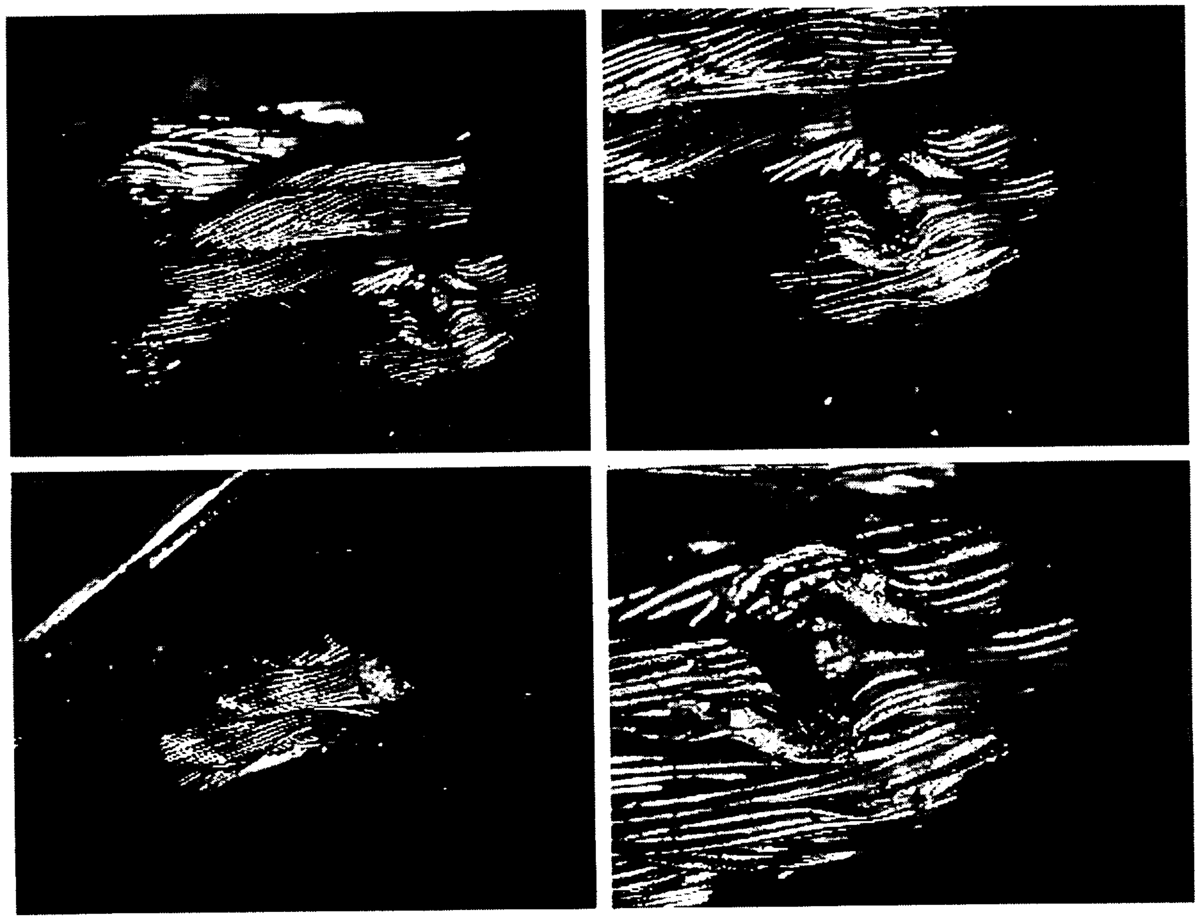

Figure 14. Physical Damage to Primary Power Lines form HIRL Shot No. A1500 at Magnifications of 6x, 10x, and 16x for Line A5B and 10x for A5A (starting upper left, going clockwise)

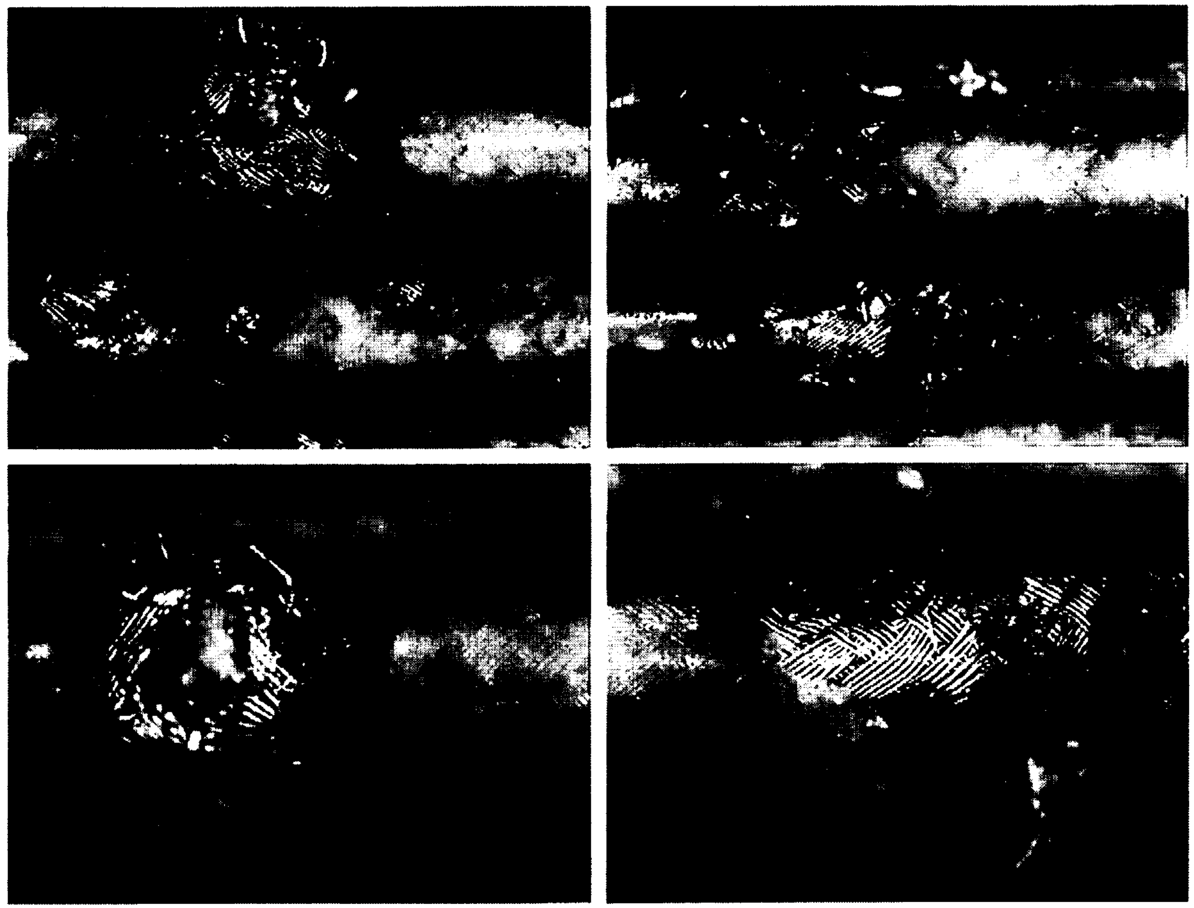

Figure 15. Physical Damage to Coaxial Line Bundle A17B from HIRL Shot No. A1509 at Magnifications of 6x, 6x, 10x, and 10x (starting upper left, going clockwise)

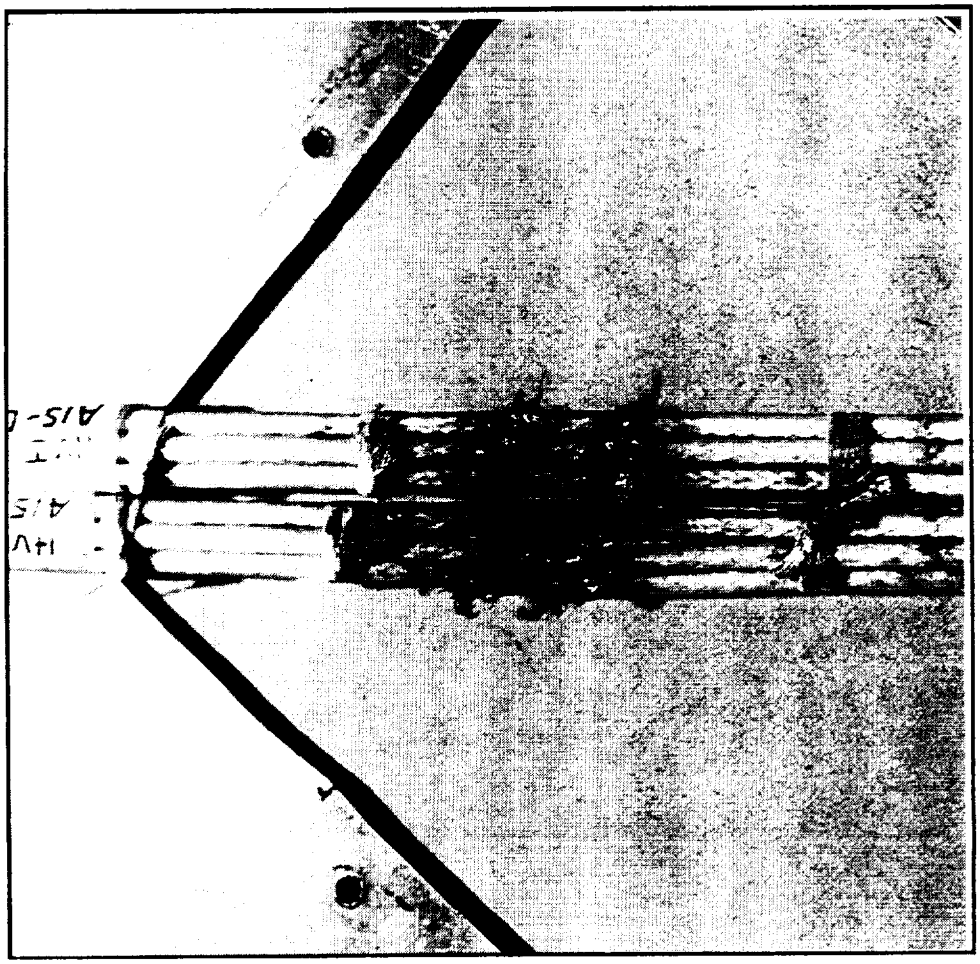

Figure 16. Physical Damage to 1553 Data Bus Lines from HIRL Shot No. A1532

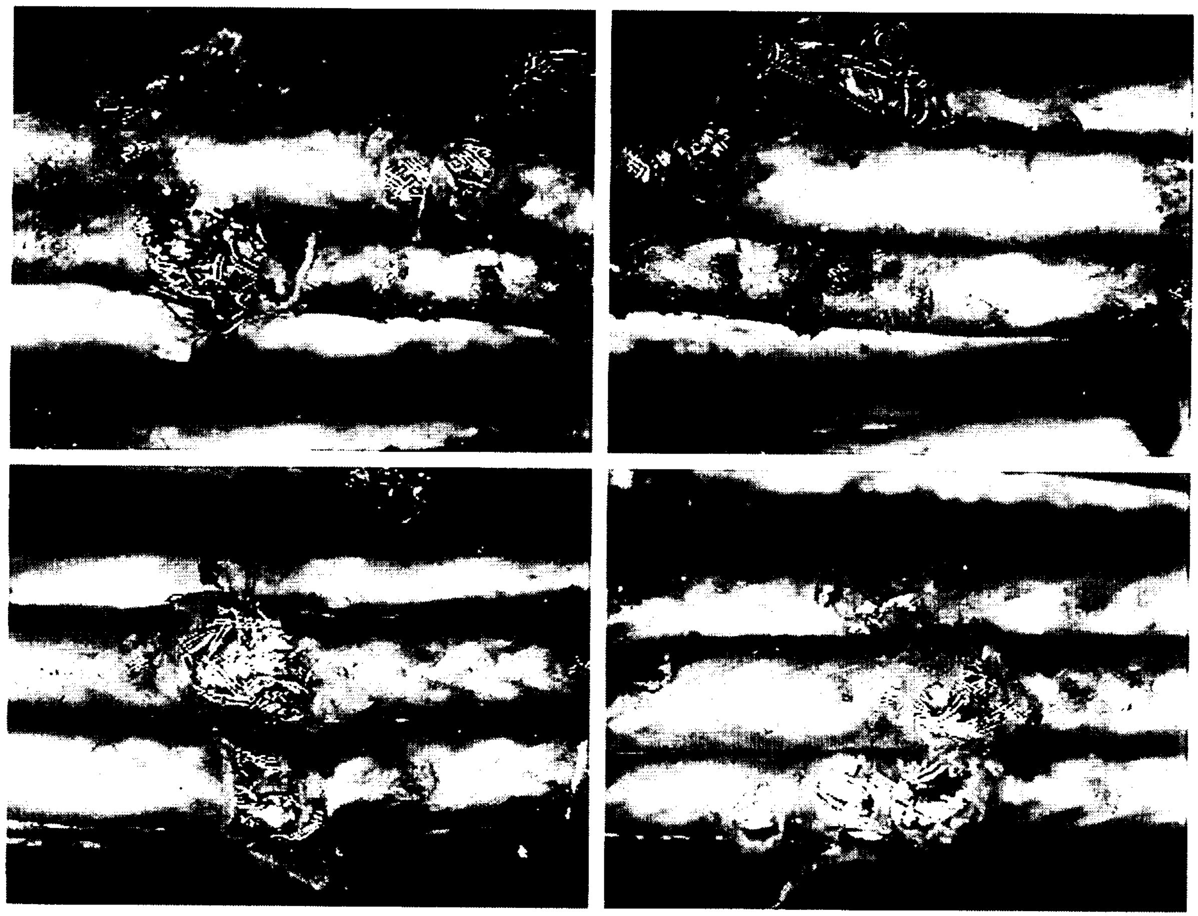

Figure 17. Physical Damage to 1553 Data Bus Lines from HIRL Shot No. A1532 at Magnifications of 6x and 6x for Line A15A and 6x and 6x for Line A15B (starting upper left, going clockwise)

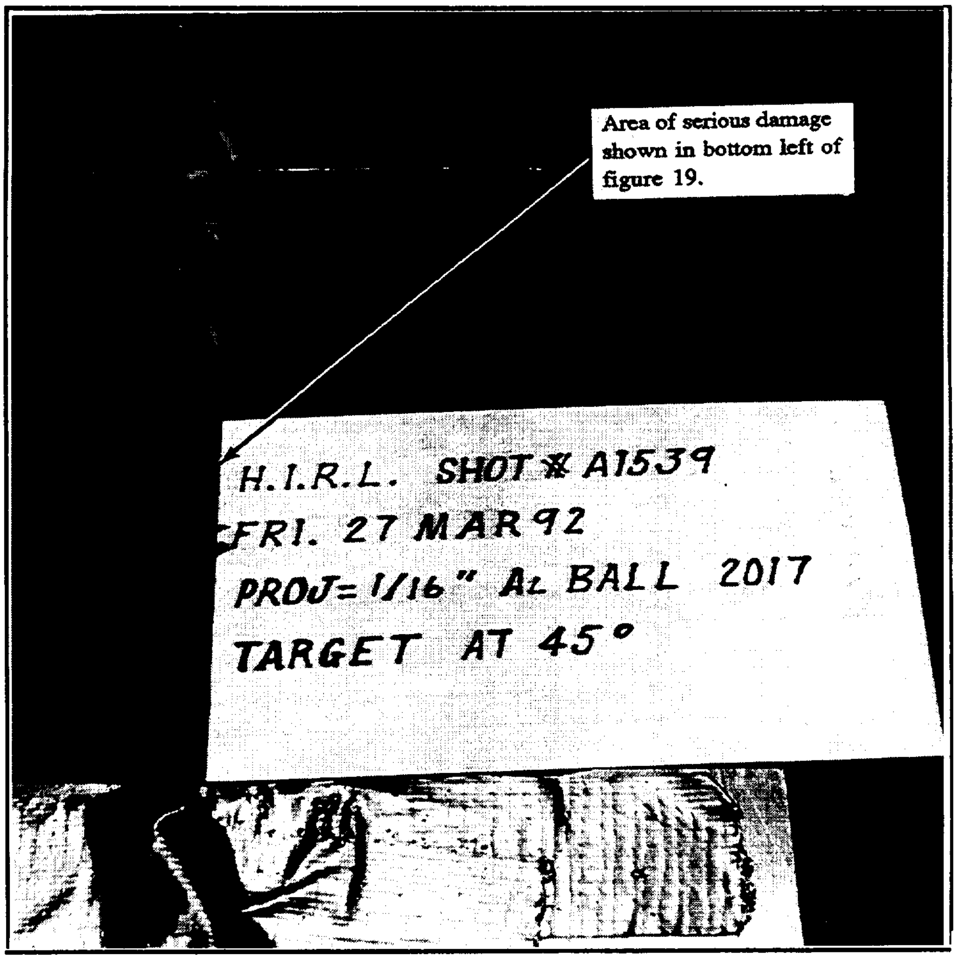

Figure 18. Physical Damage to Fiber Optic Lines from HIRL Shot No. A1539

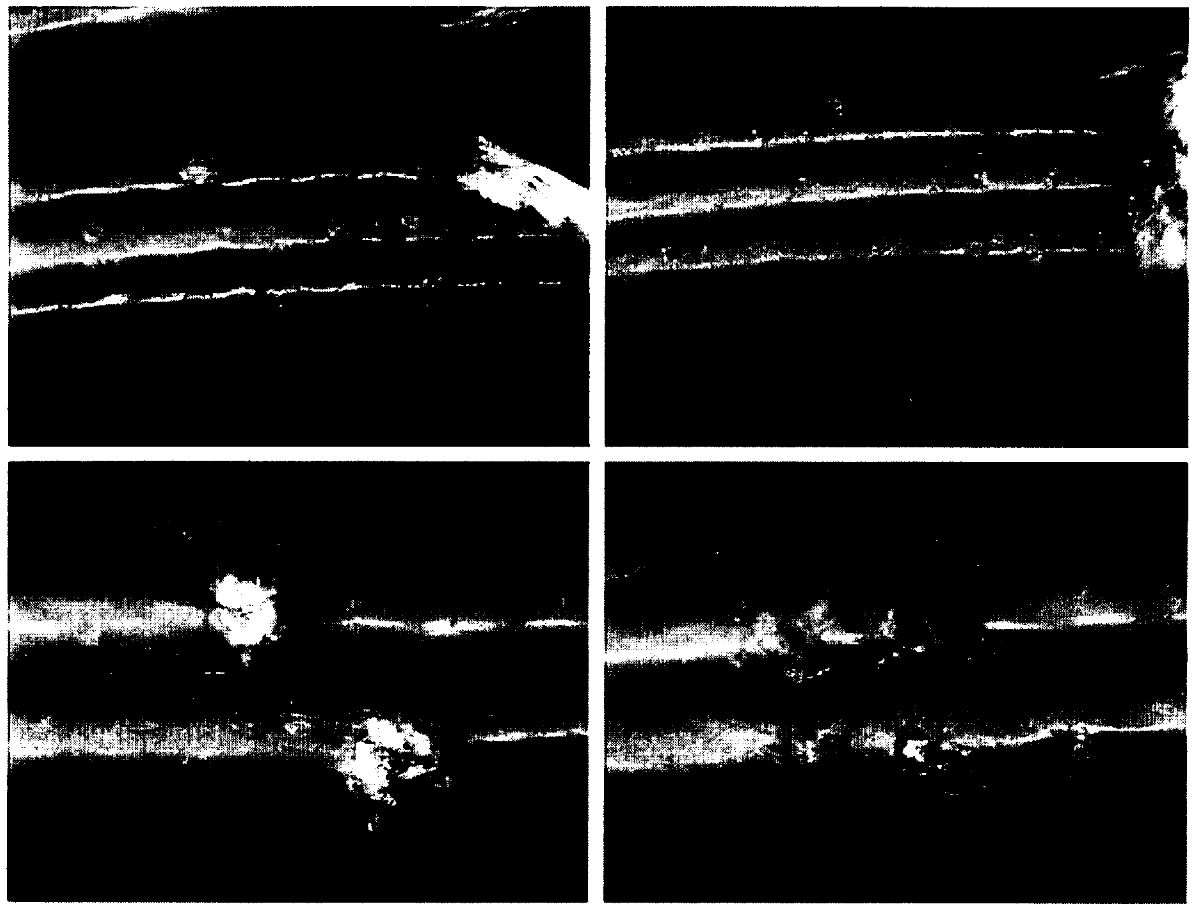

Figure 19. Physical Damage to Fiber Optic Line Bundles from HIRL Shot No. A1539 at Magnifications of 6x, 6x, 10x, and 10x (starting upper left, going clockwise)

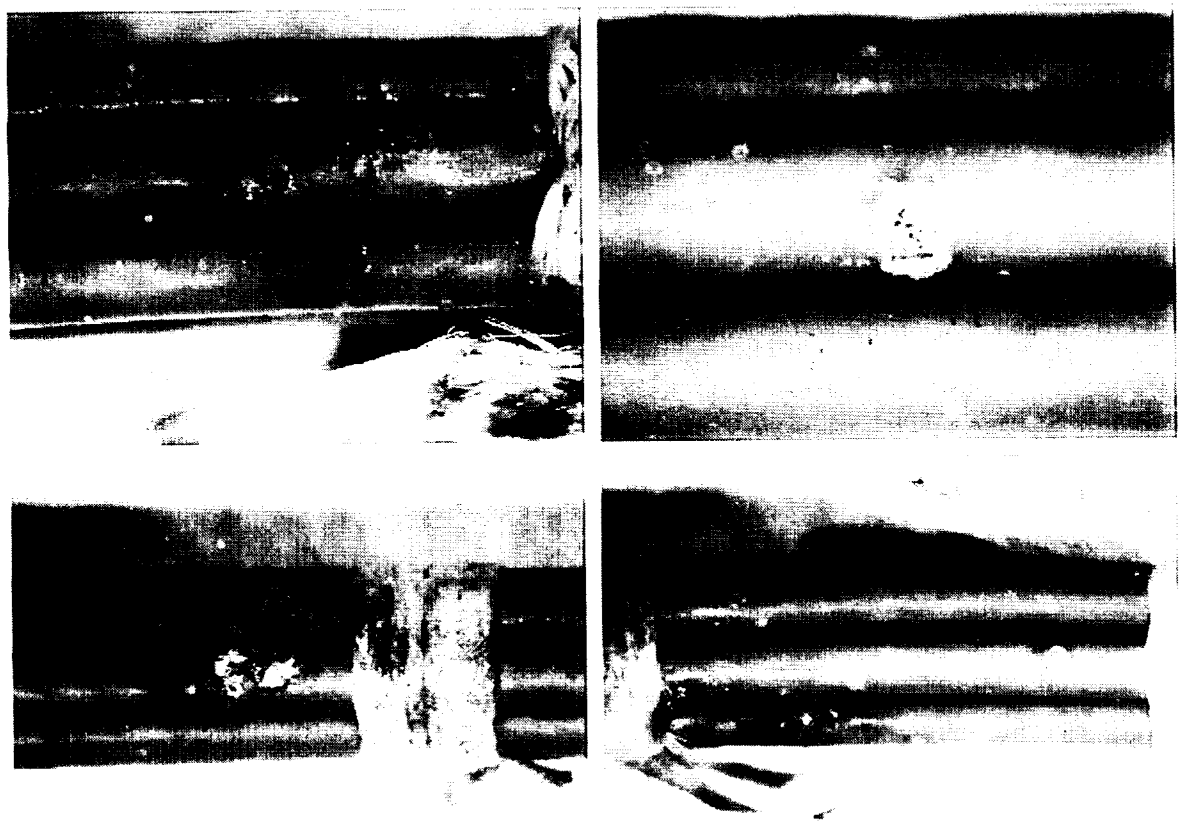

Figure 20. Physical Damage to Fiber Optic Line Bundles from HIRL Shot No. A1578 at Magnifications of 6x, 10x, 6x, and 6x (starting upper left, going clockwise)

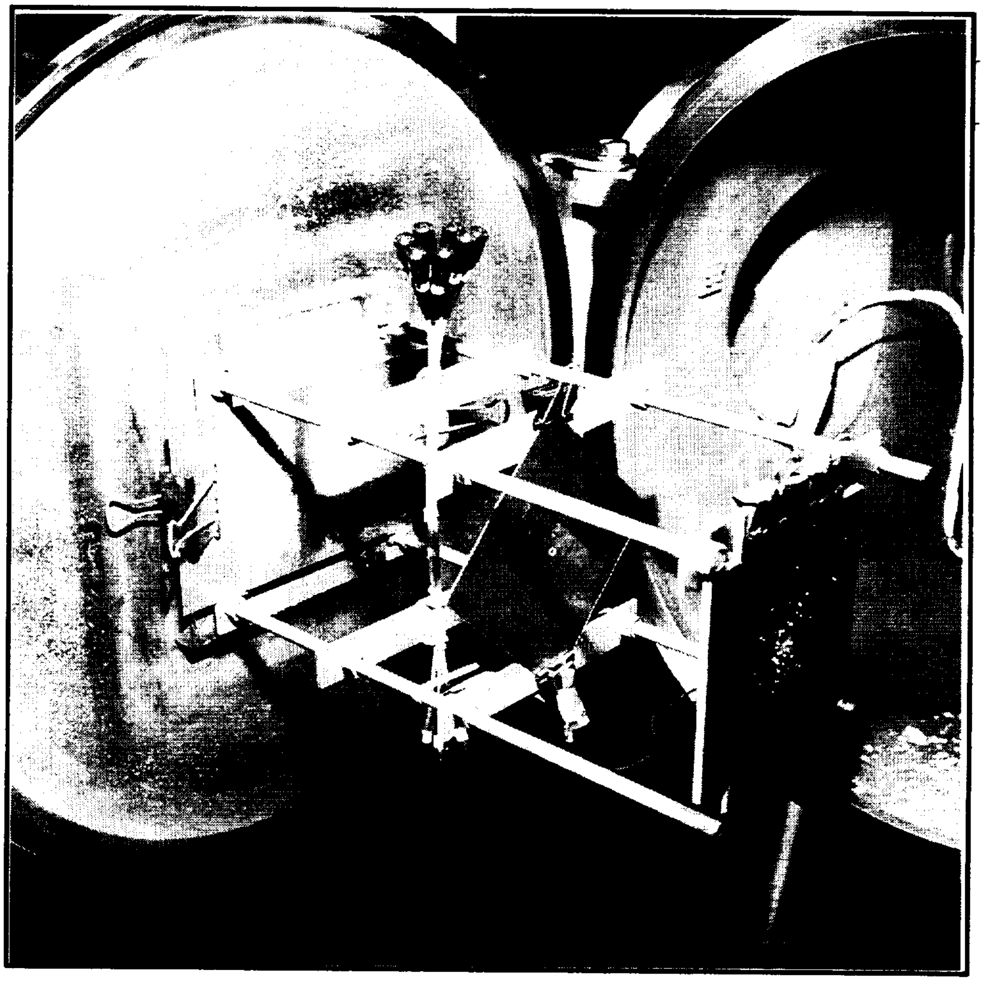

Figure 21. Bumper, Fiber Optic Bundle and Witness Plate Mounted in 1.7 mm Light Gas Gun Test Cell from HIRL Shot No. 2020

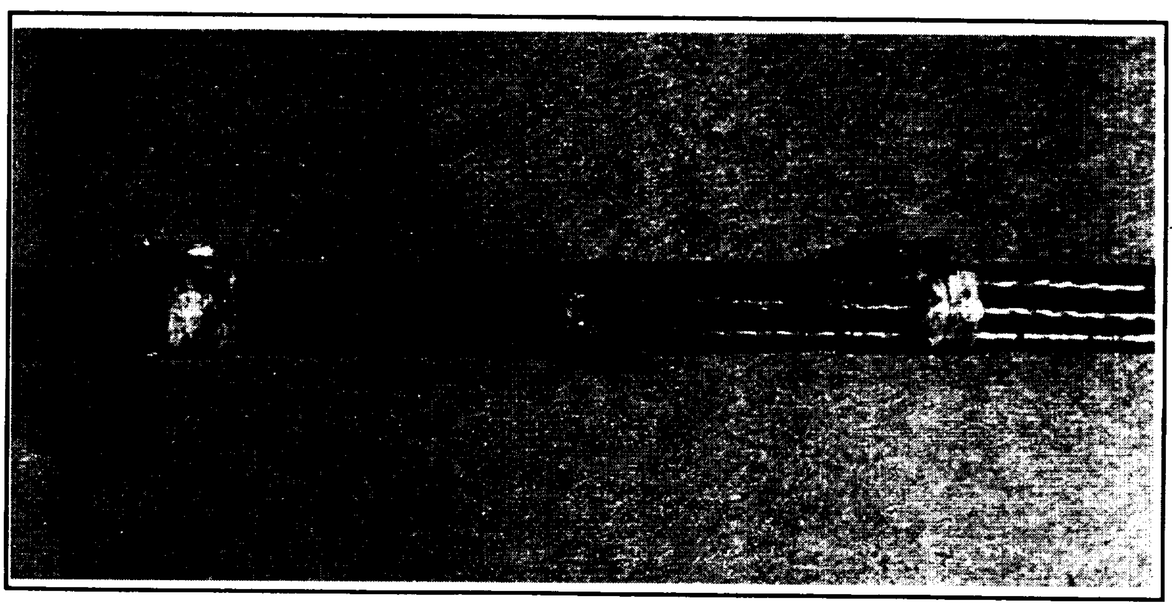

Figure 22. Physical Damage to Fiber Optic Lines from HIRL Shot No. 2020

Figure 23. Physical Damage to Active Thermal Control System Fluid Line from HIRL Shot No. A1622 at Magnification of 10x

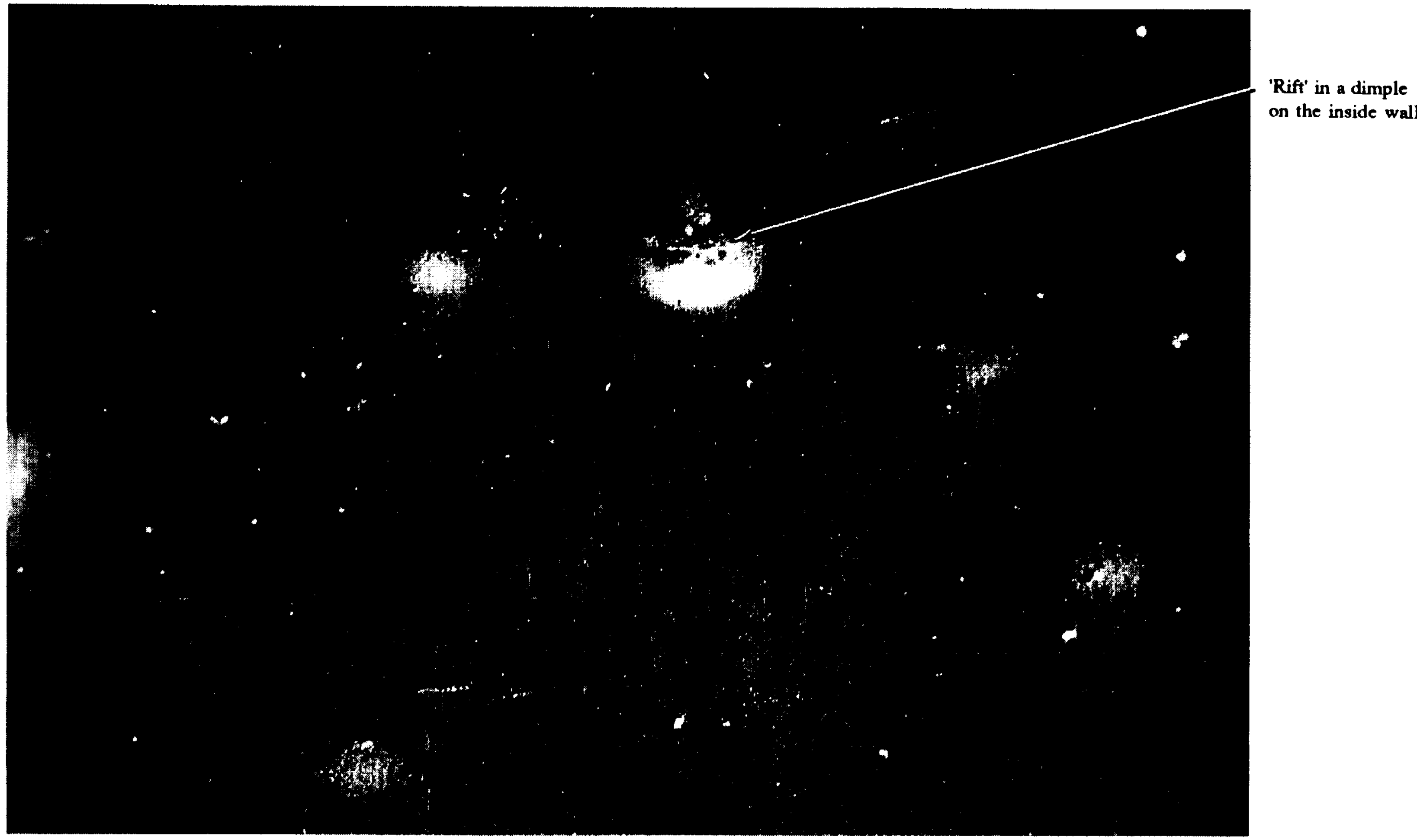

Figure 24. Physical Damage to the Internal Wall of the Active Thermal Control System Fluid Line from HIRL Shot No. A1690

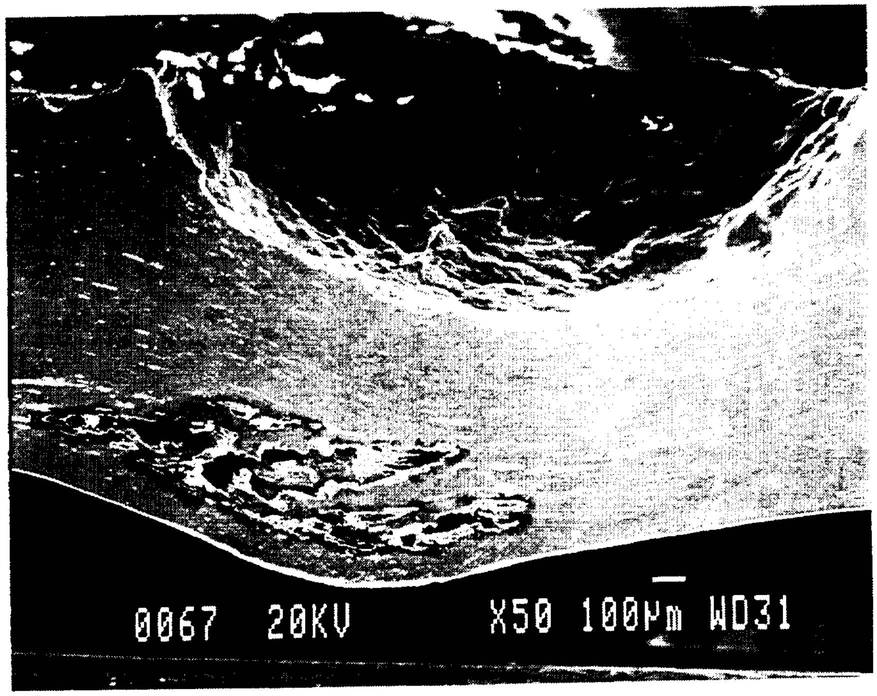

Figure 25. Scanning Electron Microscope Photo of the HIRL Shot No. A1688 TubeWall, an Impact Crater, and Inner Wall Spalling at a Magnification of 50x

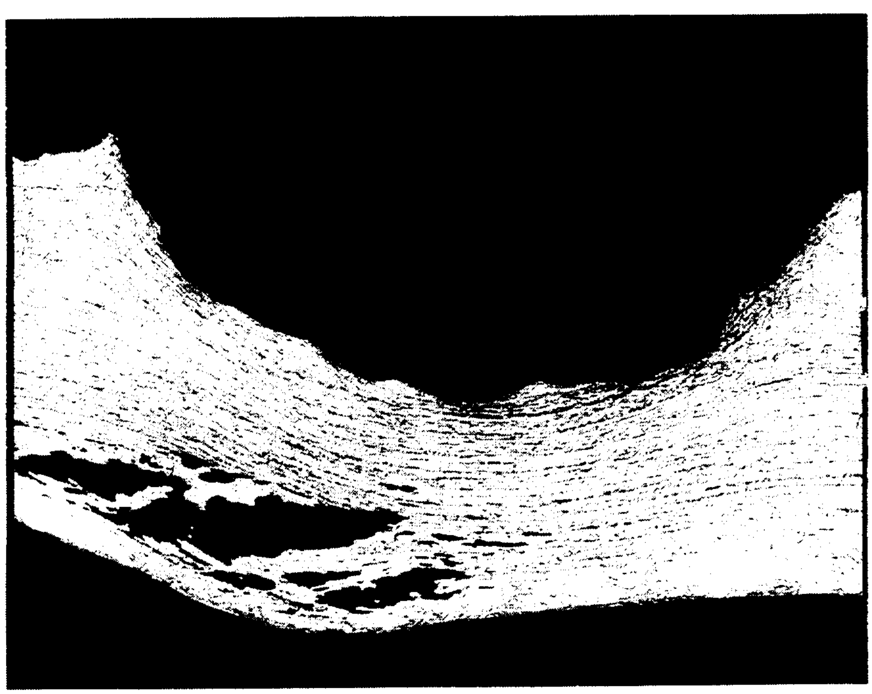

Figure 26. Metallurgical Cross Section of Fluid Line from HIRL Shot No. A1688

Figure 27. Metallurgical Cross Section of Fluid Line from HIRL Shot No. A1690

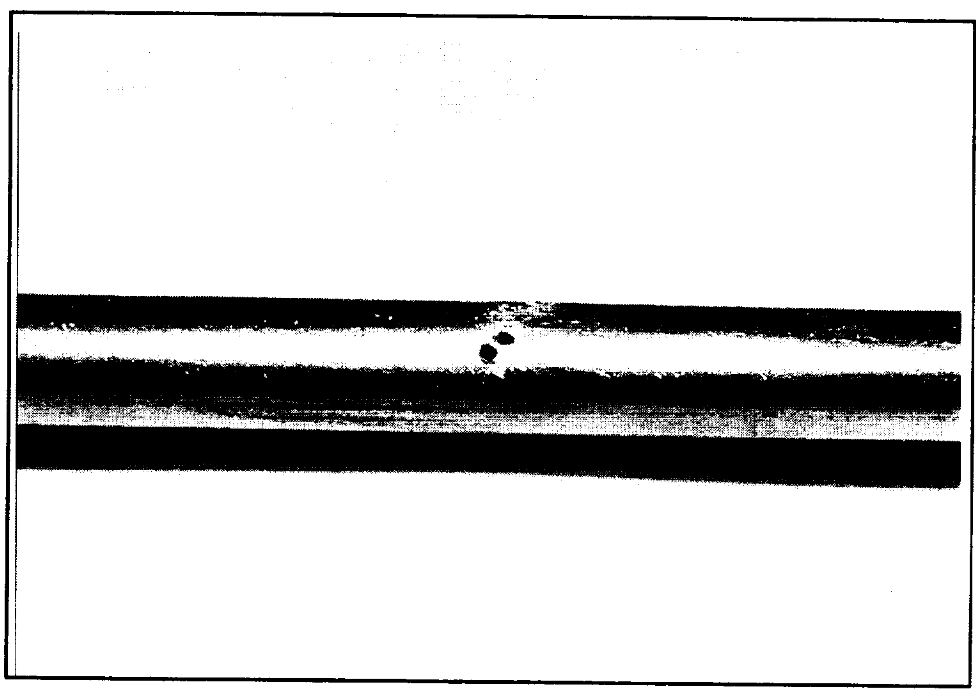

Figure 28. Physical Damage to Environmental Control and Life Support System Line from HIRL Shot No. A1631

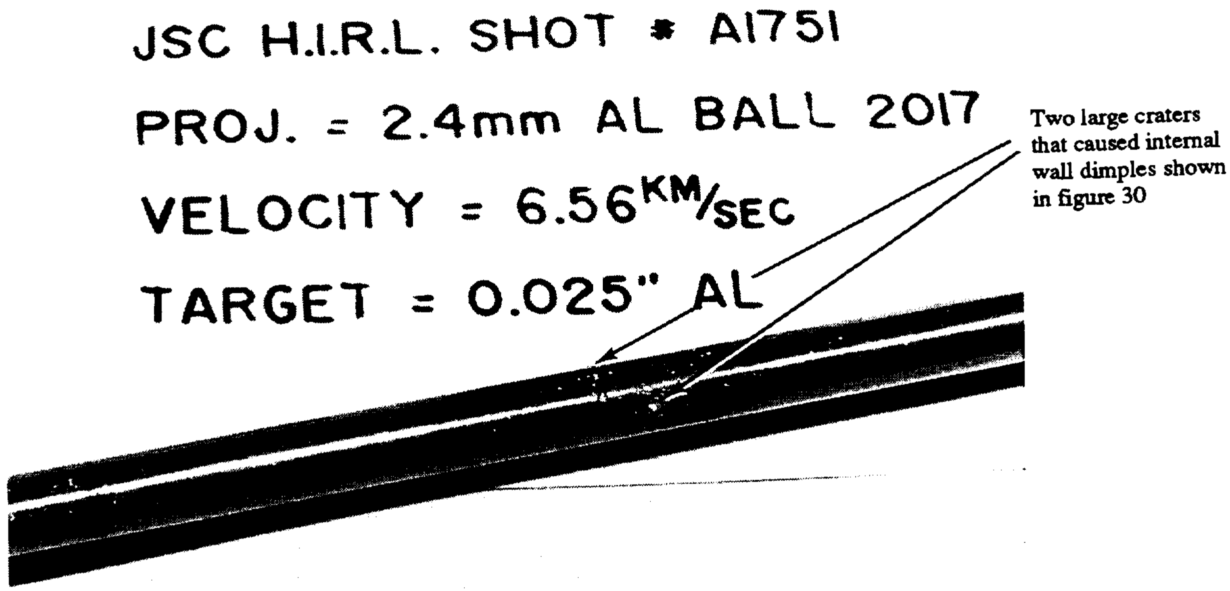

Figure 29. Physical Damage to Supplemental Reboost System Fluid Line from HIRL Shot No. A1751

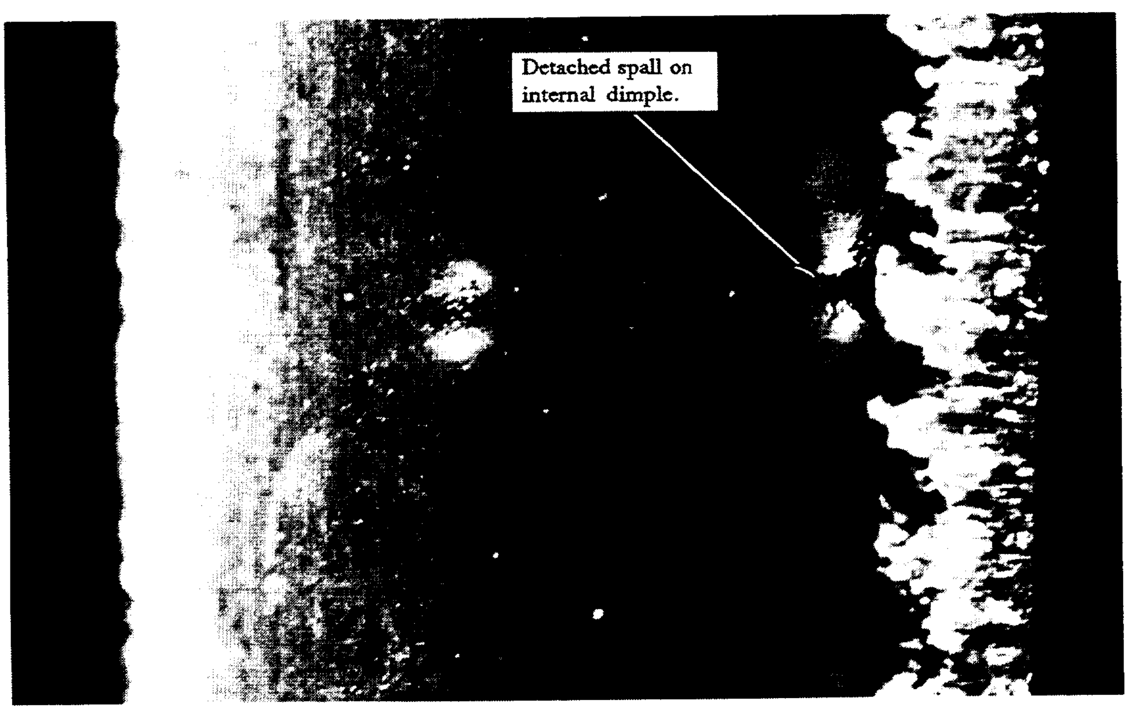

Figure 30. Close-up of Dimple on the Internal Wall of Fluid Line from HIRL Shot No. A1751

Table 1a. Projectile, Target, Bumper, and Witness Plate Descriptions from JSC HVI Tests of UDS Avionic Lines
(Shots 1940, 1941, A1492-A1494, A1498, A1500, A1505, A1507, and A1509)

JSC HIRL	DATE	PROJECTILE DESCRIPTION		TARGET DESCRIPTION			BUMPER DESCRIPTION		WITNESS PLATE DESCRIPTION	
SHOT NO.	OF SHOT	Material	Diameter	Line Type and Description	Bundle Nos.	Wire Nos.	Material/Thickness	Distance (from front of target)	Material	Distance
1940	1/21/92	Al 2017-T4	0.040 cm (1/64")	Secondary Power, Twisted Pairs, Teflon Insulated, 18 AWG Conductors, approx. 30.5 cm (12 ") long	A1A, A1C	1-7, 8-14 see notes	Al 6061-T6 t = 0.064 cm (0.025")	8.5 cm (3.35")	Al 3003-H14 t = 0.051 cm (0.020")	2.54 cm (1.0") (from back of target)
1941	1/21/92	Al 2017-T4	0.079 cm (1/32")	Secondary Power, Twisted Pairs, Teflon Insulated, 18 AWG Conductors, approx. 30.5 cm (12 ") long	A1A, A1C opp. side of test A1	1-7, 8-14 see notes	Al 6061-T6 t = 0.064 cm	8.5 cm	Al 6061-T6 t = 0.064 cm (0.025")	2.54 cm (1.0") (from back of target)
A1492	1/23/92	Al 2017-T4	0.16 cm (1/16")	Secondary Power, Twisted Pairs, Teflon Insulated, 18 AWG Conductors, approx. 30.5 cm (12 ") long	A2A, A2C	1-7, 15-21	Al 7075-T73 t = 0.064 cm	8.5 cm	Al 7075-T73 t = 0.064 cm	20.3 cm (8.0") (from back of bumper)
A1493	1/24/92	Al 2017-T4	0.24 cm (3/32")	Secondary Power, Twisted Pairs, Teflon Insulated, 18 AWG Conductors, approx. 30.5 cm (12 ") long	A1B, A2B	15-21, 8-14	Al 7075-T73 t = 0.064 cm	8.5 cm	Al 7075-T73 t = 0.064 cm	20.3 cm (8.0") (from back of bumper)
A1494	1/27/92	Al 2017-T4	0.24 cm (3/32")	Secondary Power, Twisted Pairs, Teflon Insulated, 18 AWG Conductors, approx. 30.5 cm (12 ") long	A2A, A2C opp. side of test A3	1-7, 15-21	Al 7075-T73 t = 0.064 cm	8.5 cm	Al 7075-T73 t = 0.064 cm	20.3 cm (8.0") (from back of bumper)
A1498	1/31/92	Al 2017-T4	0.32 cm (1/8")	Primary Power, Silicone Insulated, 1/0 AWG Conductor approx. 30.5 cm (12 ") long	A6A, A6B	NA	Al 7075-T73 t = 0.064 cm	8.5 cm	Al 7075-T73 t = 0.064 cm	20.3 cm (8.0") (from back of bumper)
A1500	2/4/92	Al 2017-T4	0.32 cm (1/8")	Primary Power, Silicone Insulated, 1/0 AWG Conductor approx. 30.5 cm (12 ") long	A5A,A5B, A6C	NA	Al 7075-T73 t = 0.064 cm	8.5 cm	Al 7075-T73 t = 0.064 cm	20.3 cm (8.0") (from back of bumper)
A1505	2/11/92	Al 2017-T4	0.32 cm (1/8")	Coaxial, RG-142 B/U Teflon Insulated, approx. 30.5 cm (12 ") long	A18A, A18B	1-7, 8-14	Al 7075-T73 t = 0.064 cm	8.5 cm	Al 7075-T73 t = 0.064 cm	20.3 cm (8.0") (from back of bumper)
A1507	2/13/92	Al 2017-T4	0.32 cm (1/8")	Coaxial, RG-142 B/U Teflon Insulated, approx. 30.5 cm (12 ") long	A17A, A17C	1-7, 15-21	Al 7075-T73 t = 0.064 cm	8.5 cm	Al 7075-T73 t = 0.064 cm	20.3 cm (8.0") (from back of bumper)
A1509	2/14/92	Al 2017-T4	0.24 cm (3/32")	Coaxial, RG-142 B/U Teflon Insulated, approx. 30.5 cm (12 ") long	A17B, A19A	8-14, 1-7	Al 7075-T73 t = 0.064 cm	8.5 cm	Al 7075-T73 t = 0.064 cm	20.3 cm (8.0") (from back of bumper)

Table 1b. Shot Description, Notes/Comments/Damage Descriptions, Avionic Tests, and Results of Avionic Tests from JSC HVI Tests of UDS Avionic Lines (Shots 1940, 1941, A1492-A1494, A1498, A1500, A1505, A1507, and A1509)

JSC HIRL SHOT NO.	SHOT DESCRIPTION		NOTES/COMMENTS/DAMAGE DESCRIPTION	AVIONIC TESTS	RESULTS OF AVIONIC TESTS
	Velocity (km/sec)	Angle (deg)			
1940	7.41	0	Very little physical damage to lines; small indention in insulation on wire 8; few pit marks other wires. Side exposed w/ lines (6, 1, 2) and (13, 8, 9).	Resistance and dielectric (insulation) breakdown.	No increase in resistance or change in dielectric breakdown (current leakage).
1941	6.66	0	Little physical damage; insulation marred. Several small holes/indentions in outer insulation sleeve. Side exposed w/ lines (3, 4, 5) and (12, 11, 10).	Resistance and dielectric (insulation) breakdown.	No increase in resistance or change in dielectric breakdown (current leakage).
A1492	6.97	0	Few pit marks; hole in outer insulation sleeve of line 17; did not appear to penetrate conductor's inner insulation.	Resistance and dielectric (insulation) breakdown.	No increase in resistance or change in dielectric breakdown (current leakage).
A1493	6.71	0	Large area of outer insulation sleeve damage (about 3" long.) Small damage to conductor's inner insulation; a few exposed conductor strands possible.	Resistance and dielectric (insulation) breakdown.	No increase in resistance or change in dielectric breakdown (current leakage).
A1494	6.37	45	Most severe damage concentrated over 1.5" length at top of bundles. Several areas of exposed conductor strands; some marring (black coloration and displacement) of conductor strands. 3 actual conductor strands severed. Several small holes in outer insulation continuing down lines 2.5"; a few penetrated conductor's inner insulation.	Resistance and dielectric (insulation) breakdown.	Very slight increase in resistance on wire 6.
A1498	6.42	0	Majority of damage along 2.5" length of cables; smaller amounts of marring extending an additional 1" on either side. Damage consists of small indentations/ holes/pitmarks spattered along cables; some penetration through the insulation to conductor; black coloration/burn marks along cables.	Resistance.	No increase in resistance.
A1500	6.35	45	Severe insulation damage to middle line (A5B); hole ~ 0.5" x 0.5"; some minor damage to conductor strands. Insulation damage to line A6C; potential damage to conductor. Splattering and discoloration of insulation on all lines along 4.5" of length.	Resistance.	No increase in resistance.
A1505	6.36	0	Most severe insulation damage along bundle A18B, lines 12 and 13; several holes in the shield of these lines. Large area of insulation damage along ~ 2.5" of bundles; much of this damage exposing the shield and some causing damage to the shield; discoloration (burning) of insulation.	Resistance of inner conductor and dielectric breakdown.	No increase in resistance or change in dielectric breakdown (current leakage).
A1507	6.17	45	Majority of damage centralized to 1" length of bundles. Most severe damage to lines 3, 4, 5, and 6 of A17A and line 10 of A17C. 5 & 6 have inner conductor exposed with insulation and shield ripped away; lines physically separated from each other by ~ 3/16". 4 & 10 have severe insulation and shield damage. 17 & 18 also damaged.	Resistance of inner conductor and dielectric breakdown. Note > 5mA for dielectic = arc = failure.	Several lines had significant dielectric breakdown; lines 3, 4, 5, 6, and 17 had > 5mA current leakage (arc; strands from shield close to inner conductor). Lines 5 & 6 had higher resistance (shows shield damage).
A1509	6.57	45	Majority of damage centralized to ~ 3/4" along the bundles; most severe on lines 11, 12, & 13 of A17B and 1 & 2 of A19A. Inner conductor insulation exposed on 13. Moderate shield damage to lines 11, 12, 1, and 2. Spray of small holes through insulation to shield (w/some shield damage) due to debris from bumper.	Resistance of inner conductor and dielectric breakdown.	Several lines had some minor dielectric breakdown. Line 13 was most severe with an arc detected during test (current leakage). All resistance measurements nominal.

Table 2a. Projectile, Target, Bumper, and Witness Plate Descriptions from JSC HVI Tests of UDS Avionic Lines
(Shots A1517, A1526, A1532, 2020, A1539, A1543, A1576, and A1578)

JSC HIRL	DATE	PROJECTILE DESCRIPTION		TARGET DESCRIPTION			BUMPER DESCRIPTION		WITNESS PLATE DESCRIPTION	
SHOT NO.	OF SHOT	Material	Diameter	Line Type and Description	Bundle Nos.	Wire Nos.	Material	Distance (from front of target)	Material	Distance
A1517	2/21/92	Al 2017-T4	0.24 cm (3/32")	DMS 1553 Data Bus, MIL-C-17F,M17/176-00002 Teflon Insulated, Twinax line, approx. 30.5 cm (12 ") long	A13A, A13B	1-7, 8-14	Al 7075-T73 t = 0.064 cm	8.5 cm	Al 7075-T73 t = 0.064 cm	20.3 cm (8.0") (from back of bumper)
A1526	3/3/92	Al 2017-T4	0.32 cm (1/8")	DMS 1553 Data Bus, MIL-C-17F,M17/176-00002 Teflon Insulated, Twinax line, approx. 30.5 cm (12 ") long	A14A, A14B	1-7, 8-14	Al 7075-T73 t = 0.064 cm	8.5 cm	Al 7075-T73 t = 0.064 cm	20.3 cm (8.0") (from back of bumper)
A1532	3/11/92	Al 2017-T4	0.24 cm (3/32")	DMS 1553 Data Bus, MIL-C-17F,M17/176-00002 Teflon Insulated, Twinax line, approx. 30.5 cm (12 ") long	A15A, A15B	1-7, 8-14	Al 7075-T73 t = 0.064 cm	8.5 cm	Al 7075-T73 t = 0.064 cm	20.3 cm (8.0") (from back of bumper)
2020	3/23/92	Al 2017-T4	0.16 cm (1/16")	Fiber Optic, 100/140μm type Teflon Insulated, approx. 35.6 cm (14 ") long	NA	1-7	Al 7075-T73 t = 0.064 cm	8.5 cm	Al 7075-T73 t = 0.064 cm	20.3 cm (8.0") (from back of bumper)
A1539	3/27/92	Al 2017-T4	0.16 cm (1/16")	Fiber Optic, 100/140μm type Teflon Insulated, approx. 35.6 cm (14 ") long	NA	22-28, 36-42	Al 7075-T73 t = 0.064 cm	8.5 cm	Al 7075-T73 t = 0.064 cm	20.3 cm (8.0") (from back of bumper)
A1543	4/2/92	Al 2017-T4	0.24 cm (3/32")	Fiber Optic, 100/140μm type Teflon Insulated, approx. 35.6 cm (14 ") long	NA	8-14, 29-35	Al 7075-T73 t = 0.064 cm	8.5 cm	Al 7075-T73 t = 0.064 cm	20.3 cm (8.0") (from back of bumper)
A1576	5/4/92	Al 2017-T4	0.24 cm (3/32")	Fiber Optic, 100/140μm type Teflon Insulated, approx. 35.6 cm (14 ") long	NA	57-63, 64-70	Al 7075-T73 t = 0.064 cm	8.5 cm	Al 7075-T73 t = 0.064 cm	20.3 cm (8.0") (from back of bumper)
A1578	5/6/92	Al 2017-T4	0.16 cm (1/16")	Fiber Optic, 100/140μm type Teflon Insulated, approx. 35.6 cm (14 ") long	NA	43-49, 50-56	Al 7075-T73 t = 0.064 cm	8.5 cm	Al 7075-T73 t = 0.064 cm	20.3 cm (8.0") (from back of bumper)

Table 2b. Shot Description, Notes/Comments/Damage Descriptions, Avionic Tests, and Results of Avionic Tests from JSC HVI Tests of UDS Avionic Lines (Shots A1517, A1526, A1532, 2020, A1539, A1543, A1576, and A1578)

JSC HIRL SHOT NO.	SHOT DESCRIPTION		NOTES/COMMENTS/DAMAGE DESCRIPTION	AVIONIC TESTS	RESULTS OF AVIONIC TESTS
	Velocity (km/sec)	Angle (deg)			
A1517	6.67	0	Large area of outer insulation marred (~ 2.25" long). Some penetration through outer insulation to the shield; possibly some very small damage to the shield.	Resistance of conductors and shield; dielectric breakdown for conductors and shield.	No increase in resistance or change in dielectric breakdown (current leakage).
A1526	6.20	0	Large amount of evenly distributed insulation damage along ~ 2.25" length of bundles. Some shield damage to several lines; most severe to lines 5 & 10. Debris cloud caused displacement of lines in bundles; lines 11 & 12 (right bundle; A14B) moved right, lines 3 & 4 moved left (~1/8"), line 5 moved down (~1/8") & right.	Resistance of conductors and shield; dielectric breakdown for conductors and shield.	Several lines had significant dielectric breakdown; lines 3, 4, 5, 10, and 11 had > 5mA current leakage for all dielectric checks; line 12 for only one check. All resistance measurments nominal.
A1532	6.53	45	Majority of damage centralized to ~ 3/4" along the bundles; most severe on lines 2, 3, & 4 of A15A (inner line 7 and backside line 5 also damaged) and 8, 12, & 13 of A15B. Lines 2, 4, 12, and 13 have inner conductor's insulation visible; damage to inner conductors not apparent. Very small piece of debris impacted bumper - not an issue.	Resistance of conductors and shield; dielectric breakdown for conductors and shield.	Several lines had significant dielectric breakdown; lines 2, 3, 8, and 13 had > 5mA current leakage for all dielectric checks; lines 4, 5, and 12 for two checks. All resistance measurments nominal.
2020	5.46	0	Damage spread along 3.5" of bundle; insulation marred with many pit marks; some penetrating outer jacket exposing the buffer (white fibrous material).	Light source loss along length of fiber.	No losses measured from this test.
A1539	6.75	45	Damage from particle located in middle of bundles; two small holes on lines 37 and 38; penetrated the insulation and the white fibrous buffer; possible damage to the fiber at both holes. Debris (probably piston), non-uniform shape, struck bumper 1 cm up and left of particle impact point; not an issue as to cause of test article damage.	Light source loss along length of fiber.	Significant losses in lines 37 and 38; 36.3 dB and 35.4 dB, respectively. Others showed no losses from this test.
A1543	6.73	0	Damage spread (fairly uniformly) along 3"of bundles; majority of damage insulation marring with some penetration of insulation to the buffer (white fibrous material visible on lines 32 and 33). Severe damage to lines 8 and 10; damage to insulation inner strength member and fiber; ~ half of line 8 severed.	Light source loss along length of fiber.	Total loss of light signal due to damage on lines 8 and 10. Others showed no losses from this test.
A1576	6.29	0	Damage spread along ~ 3" of bundles; majority of damage, insulation marring with some penetration of insulation to the buffer; visible especially on lines 59, 60, 66, & 68. Severe damage on lines 59, 60, 66, 68, and 69.	Light source loss along length of fiber.	Total loss of light signal due to damage on lines 59, 66, 68, and 69. Significant degradation in line 60. Others showed no losses from this test.
A1578	6.55	45	Damage from particle located in middle of bundles; one hole in line 43; one smaller hole in line 47; white fibrous material visible from line 43. Some marring on lines due to debris from both particle and bumper.	Light source loss along length of fiber.	No losses measured from this test.

Table 3a. Projectile, Target, Shot, and Bumper Descriptions from JSC HVI Tests of UDS Fluid Lines (Shots A1613, A1614, A1622, A1626, A1631, A1640, A1651, A1688, and A1690)

JSC HIRL SHOT NO.	DATE OF SHOT	PROJECTILE DESCRIPTION		TARGET DESCRIPTION	SHOT DESCRIPTION		BUMPER DESCRIPTION	
		Material	Diameter	Line Type and Description	Velocity (km/sec)	Angle (deg)	Material/Thickness	Spacing
A1613	6/16/92	Al 2017-T4	0.24 cm (3/32")	4.45 cm OD x 0.089 cm (1.75" OD x 0.035") 304L-SS; welded P = 101.3 kPa (14.7 psia) w/water	6.28	45	Al 7075-T73 t = 0.064 cm (0.025")	8.4 cm (3.3")
A1614	6/17/92	Al 2017-T4	0.32 cm (1/8")	4.45 cm OD x 0.089 cm 304L-SS; welded P = 101.3 kPa w/water	6.24	45	Al 7075-T73 t = 0.064 cm (0.025")	8.4 cm
A1622	6/24/92	Al 2017-T4	0.24 cm	4.45 cm OD x 0.089 cm 304L-SS; welded P = 101.3 kPa w/water	6.47	45	Al 7075-T73 t = 0.064 cm (0.025")	8.4 cm
A1626	6/30/92	Al 2017-T4	0.15 cm (0.059")	1.27 cm OD x 0.051 cm (0.50" OD x 0.020") 304L-SS; seamless P = 1.4 MPa (200 psia) w/GN2	6.54	45	Al 7075-T73 t = 0.064 cm (0.025")	11.2 cm (4.4")
A1631	7/13/92	Al 2017-T4	0.20 cm (0.079")	1.27 cm OD x 0.051 cm 304L-SS; seamless P = 1.4 MPa w/GN2	6.54	45	Al 7075-T73 t = 0.064 cm (0.025")	11.4 cm (4.5")
A1640	7/29/92	Al 2017-T4	0.18 cm (0.071")	1.27 cm OD x 0.051 cm 304L-SS; seamless P = 1.4 MPa w/GN2	6.54	45	Al 7075-T73 t = 0.064 cm (0.025")	11.4 cm
A1651	8/7/92	Al 2017-T4	0.20 cm	4.45 cm OD x 0.089 cm 304L-SS; welded P = 101.3 kPa w/water	6.52	45	Al 7075-T73 t = 0.064 cm (0.025")	8.0 cm (3.15")
A1688	9/10/92	Al 2017-T4	0.20 cm	4.45 cm OD x 0.089 cm 304L-SS; welded P = 101.3 kPa w/water	6.68	45	Al 7075-T73 t = 0.064 cm (0.025")	8.0 cm
A1690	9/11/92	Al 2017-T4	0.20 cm	4.45 cm OD x 0.089 cm 304L-SS; welded P = 2.0 MPa (286 psia) w/water	5.71	45	Al 7075-T73 t = 0.064 cm (0.025")	8.0 cm

Table 3b. Witness Plate Description, Bumper Damage, Damage Description of Witness Plate, and Notes/Comments/Damage Description from JSC HVI Tests of UDS Fluid Lines (Shots A1613, A1614, A1622, A1626, A1631, A1640, A1651, A1688, and A1690)

JSC HIRL SHOT NO.	WITNESS PLATE DESCRIPTION		BUMPER DAMAGE Entry Hole Size (mm)	DAMAGE DESCRIPTION OF WITNESS PLATE	NOTES/COMMENTS/DAMAGE DESCRIPTION
	Material/Thickness	Distance (from bumper)			
A1613	Al 7075-T73 t = 0.064 cm (0.025")	20.3 cm (8.0")	primary 5.0 x 6.2 mm; 2nd holes (sabot) 2.5 x 4.1mm & 1.6 x 5.2mm.	12 perforations (typ. 1.0 - 1.3 mm, 2.0 x 2.8 mm, max.); multiple small/medium craters; damage area ~ 4.6 x 5.0 cm.	Shot was off-line/debris glanced off side of tubing; no perforation of line; some internal dimpling of tube; multiple craters (typ. 0.2 - 1.2 mm); maximum crater penetration ~ 0.45, 0.56 mm. Test repeated in A1622.
A1614	Al 7075-T73 t = 0.064 cm (0.025")	20.3 cm	primary 6.0 x 7.6 mm; 2nd holes (sabot) largest 2.2 x 4.9 mm; 3.5 cm right and above primary, non-uniform shape, no affect to line.	5 perforations ranging from 0.3 mm to 1.3 x 1.8 & 1.5 x 4.3 mm; multiple craters and dimpling.	5 large perforations of tube wall (1.7, 2.3, 2.6, 2.3 x 2.8, 2.7 x 3.5 mm); several large craters; 4 internal dimples; small perforation lips; attached and detached spalls.
A1622	Al 7075-T73 t = 0.064 cm (0.025")	20.3 cm	primary 5.0 x 6.3 mm; 2nd hole 4.3x 5.0mm, non uniform shape, (piston) 0.8 cm down, 0.3 left of primary, no affect to line.	No perforations; multiple craters (typical 0.2 - 1.0 mm, 1.85 mm max.); 2 detached spalls.	2 perforations (0.85 x 1.8 and 1.52 mm); several medium craters (typical 1.2 - 1.4 mm); many small craters; some internal dimpling of tube and black soot opposite wall of perforation; detached spall.
A1626	Al 7075-T73 t = 0.064 cm (0.025")	20.3 cm	3.7 x 4.2 mm	No perforations; general scatter of small craters (0.1 -1.0 mm) and marring.	Minimal damage of line; several small craters (typical 0.1 - 0.6 mm); max. crater depth penetration ~ 0.1, 0.15 mm; ~ 2 small internal dimples.
A1631	Al 7075-T73 t = 0.064 cm (0.025")	20.3 cm	primary 4.6 x 5.4 mm; 2nd holes: 4 @ 1.0-1.1 mm; 3.7 x 4.7 mm, 7.5 cm right and down of primary, no affect to the test article.	Several small holes in witness plate (~ 17) typical size (0.5 - 1.4 mm); mulitple cratering (0.1 - 1.2 mm).	Two medium size perforations of tube wall (0.8 and 1.0 x 1.1 mm) multiple craters (0.1 - 1.3 mm; 2-4 @ upper end); max. crater penetration ~0.40 mm; couple of internal dimples.
A1640	Al 7075-T73 t = 0.064 cm (0.025")	20.3 cm	4.2 x 5.0 mm	Six small perforations in witness plate (typical 0.7 - 1.0 mm, 1.0 x 1.6 mm max.); multiple small craters (0.2 - 1.2 mm).	No penetrations of tube wall. Most of the damage is marring and craters (0.2 - 1.2 mm); one crater deeper than others (max. penetration ~ 0.41 mm). No internal dimples.
A1651	Al 7075-T73 t = 0.064 cm (0.025")	20.3 cm	primary 4.3 x 5.5 mm; 2nd hole 3.3 x 3.9 mm; 2 other very small holes. Largest just under and left of primary (piston or sabot).	3 perforations (0.1, 0.3, and 0.5 mm); multiple small craters.	No perforations of tube wall; craters typical size (0.1 - 1.4 mm); max. crater depth 0.37, 0.42 mm; several internal dimples; particle was closely followed by debris. Test repeated as A1688.
A1688	Al 7075-T73 t = 0.064 cm (0.025")	20.3 cm	primary 4.5 x 5.5 mm; 2nd hole 2.9 x 4.9 mm, 0.5 cm down and to the left (piston).	1 perforation (0.4 mm) with multiple craters (0.1 - 1.0 mm).	No perforations; multiple craters (0.2 - 1.8 mm); max. crater depth penetration 0.49, 0.64 mm; some internal dimples; piece of debris did not affect line functionally.
A1690	Al 7075-T73 t = 0.064 cm (0.025")	20.3 cm	primary 4.2 x 5.1 mm; 2nd hole 16.7 x 17.8 mm caused by piston.	3 perforations (0.3, 0.7, 0.8 mm); two large low velocity indentations (dimples) from piece of debris.	No perforations of tube wall; four large craters (max. size 2.2 mm); max. crater penetration ~ 0.38, 0.45 mm; internal dimples; spalling on internal surface (possibly detached). Piston left gaping hole in bumper.

Table 4a. Projectile, Target, Shot, and Bumper Descriptions from JSC HVI Tests of UDS Fluid Lines (Shots A1693, A1695, A1749-A1751, and A1800)

JSC HIRL SHOT NO.	DATE OF SHOT	PROJECTILE DESCRIPTION		TARGET DESCRIPTION	SHOT DESCRIPTION		BUMPER DESCRIPTION	
		Material	Diameter	Line Type and Description	Velocity (km/sec)	Angle (deg)	Material/Thickness	Spacing
A1693	9/18/92	Al 2017-T4	0.20 cm	1.27 cm OD x 0.051 cm (0.50" OD x 0.020") 304L-SS; seamless P = 101.3 kPa (14.7 psia) w/GN2	6.60	45	Al 7075-T73 t = 0.064 cm (0.025")	11.4 cm (4.5")
A1695	9/21/92	Al 2017-T4	0.18 cm	1.27 cm OD x 0.051 cm 304L-SS; seamless P = 101.3 kPa w/GN2	6.54	45	Al 7075-T73 t = 0.064 cm (0.025")	11.4 cm
A1749	10/27/92	Al 2017-T4	0.18 cm	1.27 cm OD x 0.051 cm 304L-SS; seamless P = 101.3 kPa w/GN2	6.42	45	Al 7075-T73 t = 0.064 cm (0.025")	11.4 cm
A1750	10/27/92	Al 2017-T4	0.20 cm	0.95 cm OD x 0.089 cm (0.375" OD x 0.035") 304L-SS; seamless P = 6.9 MPa (1000 psia) w/ GN2	6.31	45	Al 7075-T73 t = 0.064 cm (0.025")	11.7 cm (4.6")
A1751	10/28/92	Al 2017-T4	0.24 cm (3/32")	0.95 cm OD x 0.089 cm 304L-SS; seamless P = 6.9 MPa w/ GN2	6.56	45	Al 7075-T73 t = 0.064 cm (0.025")	11.7 cm
A1800 (repeat of A1690)	1/5/93	Al 2017-T4	0.20 cm	4.45 cm OD x 0.089 cm 304L-SS; welded P = 2.0 MPa w/water	6.69	45	Al 7075-T73 t = 0.064 cm (0.025")	8.0 cm

Table 4b. Witness Plate Description, Bumper Damage, Damage Description of Witness Plate, and Notes/Comments/Damage Description from JSC HVI Tests of UDS Fluid Lines (Shots A1693, A1695, A1749-A1751, and A1800)

JSC HIRL SHOT NO.	WITNESS PLATE DESCRIPTION Material/Thickness	Distance (from bumper)	BUMPER DAMAGE Entry Hole Size (mm)	DAMAGE DESCRIPTION OF WITNESS PLATE	NOTES/COMMENTS/DAMAGE DESCRIPTION
A1693	Al 7075-T73 t = 0.064 cm (0.025")	20.3 cm	4.4 x 5.4 mm	One large perforation (1.1 x 2.0 mm) and three smaller perforations (0.5, 0.6, 0.7 mm); multiple craters (0.1 - 1.0 mm).	One small perforation (0.6 x 0.7 mm); ~ 11 craters (typical size 0.5 - 1.0 mm); no internal dimples.
A1695	Al 7075-T73 t = 0.064 cm (0.025")	20.3 cm	primary 4.1 x 4.7 mm; 2nd hole 2.3 x 3.4 mm, 0.5 cm above the primary, (piston) non-uniform hole.	2 small perforations (0.3 and 0.4 mm) with multiple craters (typical 0.1 - 1.3 mm); not all target and projectile debris impacted witness plate (went above witness plate).	One perforation (1.1 x 1.6 mm); could have been caused by test particle or by piece of debris following particle. Test will be REPEATED.
A1749	Al 7075-T73 t = 0.064 cm (0.025")	20.3 cm	4.2 x 4.9 mm	11 perforations (typ. 0.1 -1.0 mm, 1.3 mm max); multiple craters and dimples (0.1 - 1.4 mm)	REPEAT of A1695. No perforation of tube wall; damage is marring and small craters (0.1 - 1.5 mm)-- similar to results of A1640. Max. crater penetration ~ 0.12 mm.
A1750	Al 7075-T73 t = 0.064 cm (0.025")	20.3 cm	primary 4.4 x 5.2 mm; 2nd holes 2.6 x 2.8 mm, under and left of primary, piece of piston; 1.1 x 2.9 mm; two other small ones.	11 perforations; six at 0.6 - 0.8 mm; four larger at 1.4, 1.5, 1.6, and 1.9 mm; multiple craters and dimpling.	No perforation of tube wall; multiple craters (typical 0.1 - 1.3 mm, 0.9 x 1.6 mm max); max crater penetration ~ 0.3 mm. Piston did not affect line.
A1751	Al 7075-T73 t = 0.064 cm (0.025")	20.3 cm	primary 5.0 x 6.1 mm; 2nd hole 4.5 x 6.6mm, 1 cm right and 1.5 cm down from primary, non-uniform shape (piston), no affect to line.	~ 19 perforations (typical 0.3 - 1.2 mm); five larger at 1.4, 1.8, 1.0 x 1.7, 1.5 x 2.3 and 2.5 mm and multiple craters.	No perforation of tube wall; multiple craters (typical 0.1 - 1.7 mm, max 1.8 x 2.7 mm); max crater penetration 0.29, 0.35 mm; ~ 3 internal dimples with potential of one having detached spall.
A1800	Al 7075-T73 t = 0.064 cm (0.025")	20.3 cm	4.5 x 5.1 mm	1 perforation (0.1 mm); multiple craters	No perforations of tube wall; three large craters; several internal dimples, four large.

APPENDIX A: DATA FOR THE UDS AVIONIC LINES USED FOR HVI TESTING

1553 Data Bus Cable (MIL-C-17F, M17/176-00002)

Twisted, shielded pair

Inner conductors:	Two 24 American wire gage (AWG) consisting of 19 strands of 36 AWG silver-coated, high strength copper alloy
Outer conductor:	Single braid of 38 AWG silver-coated, high strength copper alloy wire
Jacket:	PFA; Diameter 0.129 ± 0.005 in.

Primary Power

1/0 AWG line conductor

Cable diameter:	0.545 ± 0.010 in.
Conductor:	Class N, nickel-coated, stranded copper rope lay
Insulation:	Silicone

Secondary Power

Twisted pair, unshielded and unjacketed

Cable diameter:	0.150 in.
Conductors:	18-gage stranded conductors
Insulation:	Teflon

Coaxial Cable (RG-142B/U)

Inner conductor:	Solid silver-coated, copper-covered steel wire
Dielectric core:	Solid extruded PTFE (inner conductor insulation)
Outer conductor:	Double braid of 36 AWG silver-coated copper wire
Jacket:	Teflon FEP; Diameter 0.195 ± 0.005 in.

Fiber Optic Cable

100/140 μm type (core = 100 μm, cladding = 140 μm)

Cable diameter:	0.083 ± 0.002 in.
Optical fiber:	Doped silica (glass)
Protective coating:	High temperature polymide compound
Tube:	Teflon FEP
Strength member:	Braided teflon coated fiberglass
Jacket:	Teflon FEP

APPENDIX B: PRE-HVI AND POST-HVI AVIONIC LINE FUNCTIONAL CHECKOUT DESCRIPTION

These checkouts were conducted before each HVI test and then hand carried to the HIRL. After the HVI test was completed, the test articles were returned to the EPS lab and these checkouts were repeated. This allowed the current carrying "health" of the lines to be determined.

The functional checks for the power, 1553 data bus, and coaxial lines were performed at the EPS Laboratory in building 16 at JSC. The test equipment used for this part of the program are as follows:

1) Slaughter Series 103/105 Dielectric Breakdown and Leakage Tester

2) Hewlett-Packard Model 3456A Digital Multimeter

3) Valhalla Scientific 2555A AC-DC Current Calibrator

4) Valhalla Scientific 4300B Digital Micro-ohmmeter

5) Fluke 343A DC Voltage Calibrator

The functional checks for the fiber optic lines were performed at the Fiber Optic Test Bench in building 15 at JSC. The test equipment used for this part of the program are as follows:

1) Noyes Optical Light Source OLS1-2

2) Noyes Optical Power Meter OPM1-2

PRIMARY POWER LINE CHECKOUT

Resistance Test: Each test article was connected as shown in figure B1. The insulation on a test article was fitted against the test blocks and the four bolts were torqued down to 134 inch pounds (this provided a good tight contact without crushing the wires). The Fluke 343A DC Voltage Calibration Source was set to 1 volt and the Valhalla 4300B micro-ohmmeter was set to test at 2 volts at 10 A. The resistance was then recorded from the Valhalla 4300B.

SECONDARY POWER LINE CHECKOUT

Resistance Test: Each conductor of the test article was connected as shown in figure B2. The Valhalla 4300B micro-ohmmeter was set to 200 millivolts and 10 A (with no temperature compensation being used). The test was initiated and after one minute, the reading was recorded. This time allowed the test article to settle after experiencing any initial minor transient or heating effects.

Dielectric Breakdown Test: The Slaughter 103/105 Dielectric Breakdown and Leakage Tester was set to the DC position, the voltage regulator to the X1 position and a 1200 volts voltage limit, and the current meter to the X1 position and a 100 μA limit. The timer was set for 30 seconds. The conductor under test was then connected to the positive side of the tester while all remaining conductors in the test article bundle were connected to the return side. The power was turned on and the Slaughter 103/105 was set to auto mode. The test was initiated and any current leakage measured on the current meter was recorded. If the arc indicator light turned on, this signified that the tester detected a current leakage of greater than 5 mA. For the purposes of this phase of the test program, this current leakage constituted a failure of the line. This test was performed for each conductor of the test article.

1553 DATA BUS LINE CHECKOUT

Resistance Test of Inner Conductors: This test is identical to the resistance test for the secondary power lines except that the Valhalla 4300B micro-ohmmeter was set to 1 A.

Resistance Test of Shield: This test is identical to the resistance test for the secondary power lines except that the Valhalla 4300B micro-ohmmeter was set to 20 millivolts and 1 A.

Dielectric Breakdown Test: This test is identical to the dielectric breakdown test for the secondary power lines except the voltage regulator was set to a 1000 volts voltage limit.

COAXIAL LINE CHECKOUT

Resistance Test of Inner Conductors: This test is identical to the resistance test for the secondary power lines except that the Valhalla 4300B micro-ohmmeter was set to 20 millivolts and 1 A.

Resistance Test of Shield: This test is identical to the resistance test for the secondary power lines.

Dielectric Breakdown Test: This test is identical to the dielectric breakdown test for the secondary power lines except the voltage regulator was set to a 1400 volts voltage limit.

FIBER OPTIC LINE CHECKOUT

Light Transmission Degradation Test: Before each fiber optic line was checked, a specific procedure was performed as shown in figure B3. The Noyes Optical Power Source and Optical Light Meter were set for a wavelength of 1.3μm. A launch cable was attached and a reading taken, reading X. The launch cable is a special fiber optic line with a calibrated attenuation and is used to establish a baseline loss measurement for the checkouts that will be performed. Because the light source and meter could not be physically connected to obtain this measurement, the launch cable was required.

Next, a reading was taken for each fiber optic line test article, reading Y, using the configuration shown in figure B4. The launch cable is required here to insure that the baseline loss measurement, established above, is maintained. Finally, reading Y is subtracted from reading X to obtain the losses for the fiber optic line test article.

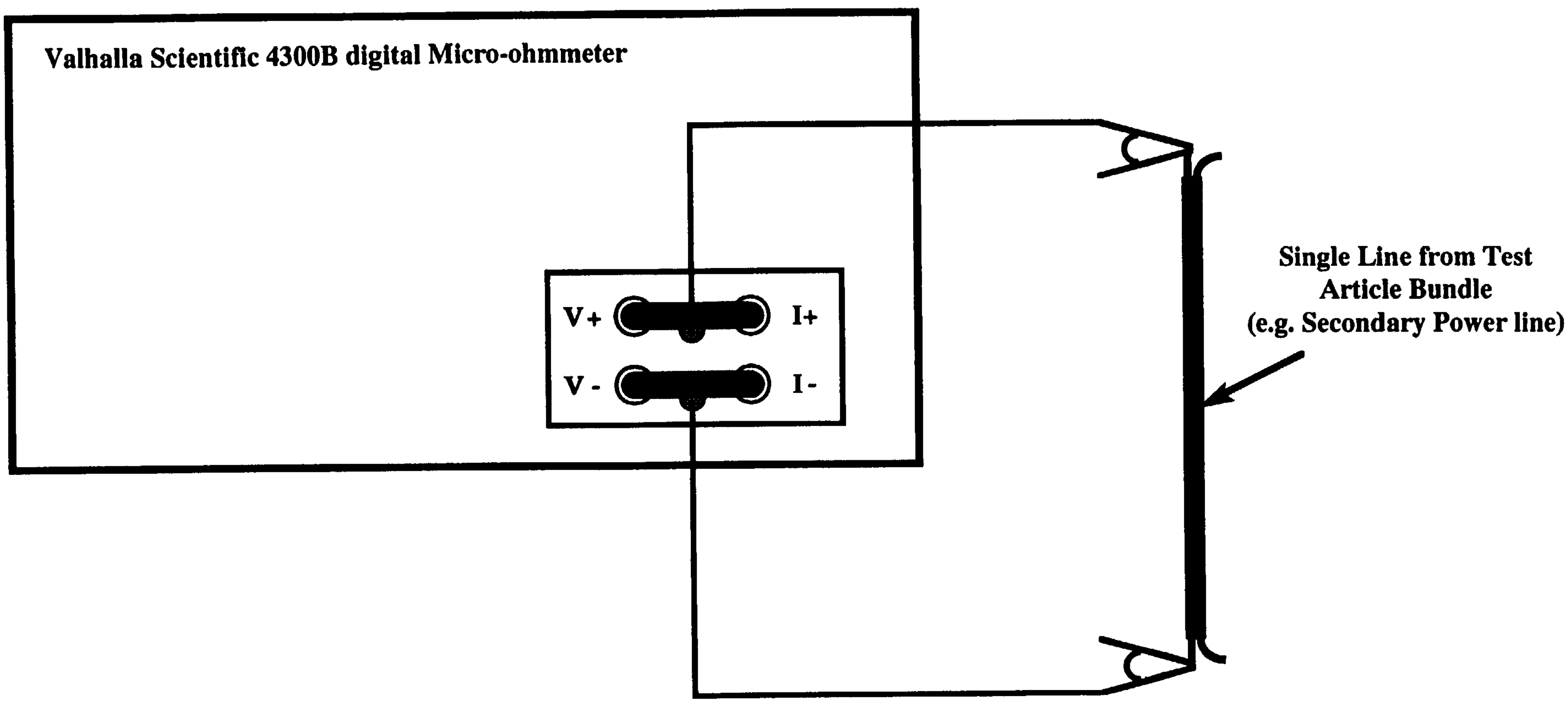

Figure B1. Setup for Resistance Check of Secondary Power, Coaxial, and 1553 Data Bus Lines

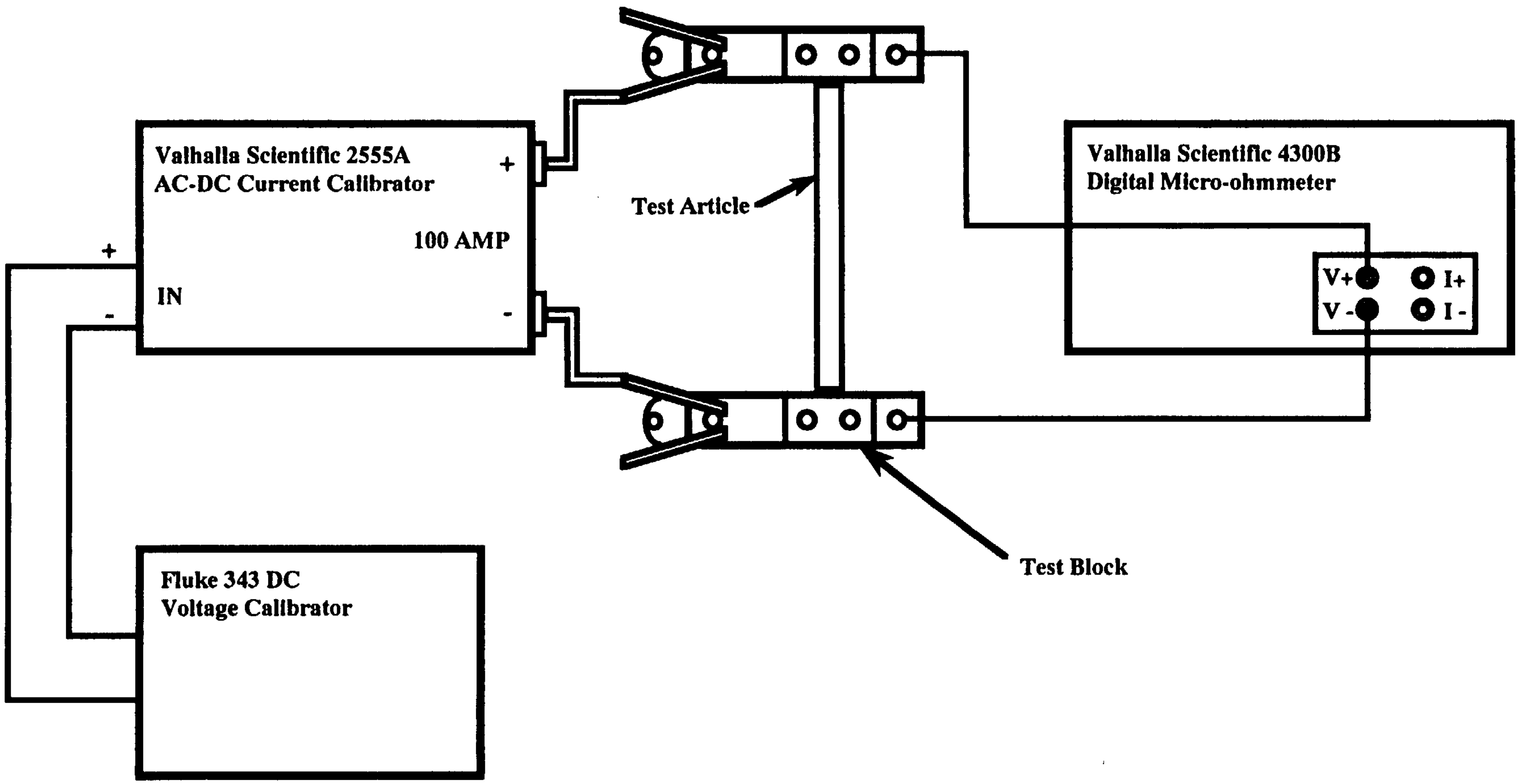

Figure B2. Setup for Resistance Check of Primary Power Lines

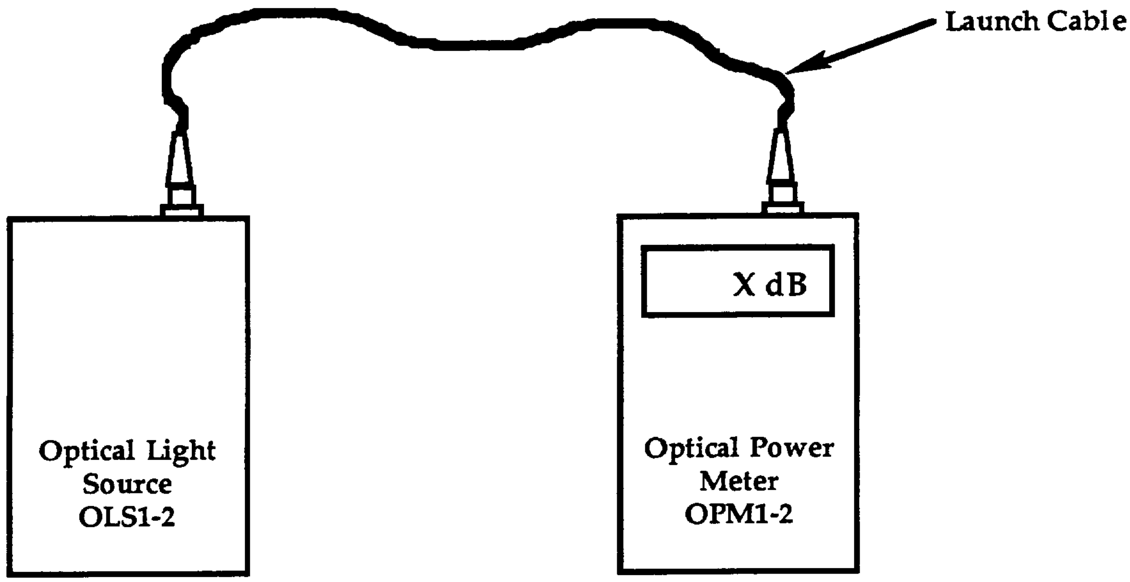

Figure B3. Setup for Establishment of Fiber Optic Cable Baseline Conditions

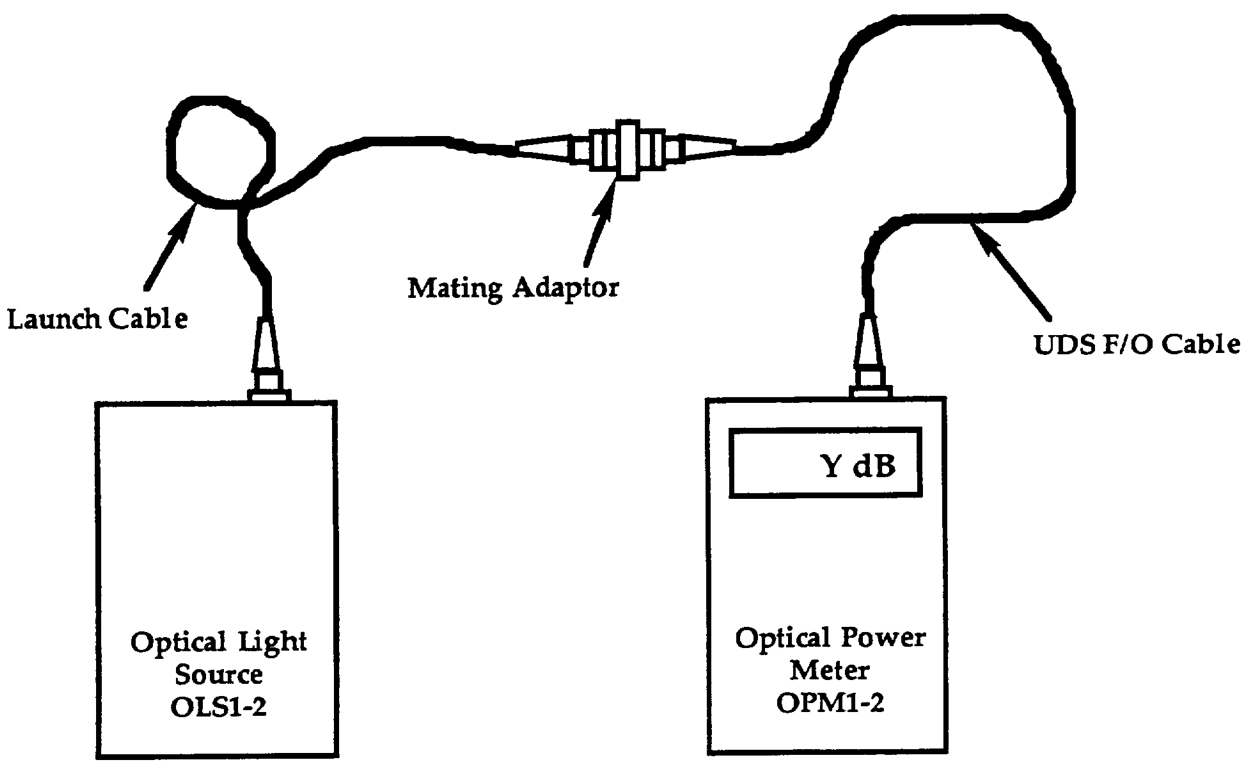

Figure B4. Setup for Determining Losses in Fiber Optic Cable

APPENDIX C: LIST OF NASA PHOTOGRAPHS FROM TEST PROGRAM

Avionic Lines

HIRL Shot No.	Photo No.
1940	S92-27131 - S92-27136
1941	S92-27392 - S92-27396
A1492	S92-27125 - S92-27130
A1493	S92-27178 - S92-27184
A1494	S92-27397 - S92-27399
A1498	S92-28248 - S92-28251
A1500	S92-27914 - S92-27917
A1505	S92-28274 - S92-28277
A1507	S92-28311 - S92-28313
A1509	S92-29010 - S92-29013
A1517	S92-29006 - S92-29009
A1526	S92-29724 - S92-29728
A1532	S92-31113 - S92-31117
2020	S92-32079 - S92-32082
A1539	S92-32519 - S92-32521
A1543	S92-32758 - S92-32759
A1576	S92-36091 - S92-36094
A1578	S92-36095 - S92-36098

Fluid Lines

HIRL Shot No.	Photo No.
A1613	S92-39034 - S92-39036
A1614	S92-39037 - S92-39040
A1622	N/A
A1626	S92-41718 - S92-41721
A1631	S92-41715 - S92-41717, S92-41722
A1640	N/A
A1651	S92-43375 - S92-43380
A1688	S92-47372 & S92-47375
A1690	S92-47371 & S92-47374
A1693	S92-47368 & S92-47369
A1695	S92-47370 & S92-47373
A1749	S92-49389 - S92-49392
A1750	S92-49381 - S92-49384
A1751	S92-49385 - S92-49388

APPENDIX D: BUMPER-E VULNERABILITY ANALYSIS OF THE UDS TRAYS

Lockheed
Engineering & Sciences Company

ENGINEERING AND SCIENCE PROGRAM
2400 NASA Road 1, P. O. Box 58561, Houston, Texas 77258-8561
713-333-5411

March 30, 1992
MDS-505

To: Scott Lazaroff/NASA-JSC/EP53

Via: Eric Christiansen/NASA-JSC/SN3
Robert Franson/LESC/B22 REF
Demos Tsairides/LESC/B22 DT

From: James L. Hyde/LESC/B22
Gillian L. Shephard/LESC/B30

Subject: **PREDICTED NUMBER OF METEOROID AND DEBRIS IMPACTS ON THE UTILITY DISTRIBUTION SYSTEM (UDS) TRAY**

Please find attached the preliminary results of our BUMPER-E vulnerability analysis of the UDS trays. The predictions are based on a finite element model (FEM) of the full UDS tray in the PMC configuration (LVLH attitude). The FEM was developed from a design sketch titled "PIT UTILITY CARRIERS -- FLAT PATTERN." Table 1 lists the tray dimensions that were shown in the sketch. Table 2 gives probability of no impact (PNI) and expected number of impacts on the avionics and fluids sections for seven test particle diameters. The "energy scaled diameters" shown in the second and third columns of table 2 were calculated using the equations 1 and 2.

Meteoroids: $$d_{eq} = d_{test} \times \left(\frac{6.5}{20}\right)^{2/3} \times \left(\frac{2.8}{\rho}\right)^{1/3} \qquad \text{(Eq. 1)}$$

Where $\rho = 0.5$ g/cc for 3/8", 1/4" & 1/8" particles and 1.0 g/cc for others...

Debris: $$d_{eq} = d_{test} \times \left(\frac{6.5}{10}\right)^{2/3} \qquad \text{(Eq. 2)}$$

The results of this analysis should be classified as preliminary. Additional runs should be made at typical SSF attitudes and a time-average prediction made for the expected number of impacts. The BUMPER PNI code does not predict number of failures. It should be noted that one impact event could cause multiple failures in the utility tray. A more refined analysis will be performed in the future.

James L. Hyde
James L. Hyde
Structures and Mechanics Department

Gillian L. Shephard
Gillian L. Shephard
Structures and Mechanics Department

Table D1. UDS Tray Dimensions

tray segment	region	length (in)	compartment width (in) face 2 (upper)			compartment width (in) face 6 (lower)		
			avionics	fluids	total	avionics	fluids	total
S3	B1	97.110	12.0	0.0	**12.0**	12.0	0.0	**12.0**
	B2	104.470	21.0	3.7	**24.7**	20.0	3.7	**23.7**
S2	B1	91.950	21.0	9.0	**30.0**	20.0	9→11.5	-
	B2	80.430	21.0	9.0	**30.0**	17.5	11.5	**29.0**
	B3	53.310	21→33	9.0	-	17.5→33	11.5	-
	B4	54.310	33.0	9.0	**42.0**	33.0	11.5	**44.5**
S1	B1	101.200	33.0	9.0	**42.0**	33.0	11.5	**44.5**
	B2	100.420	33.0	9.0	**42.0**	33.0	11.5	**44.5**
	B3	101.380	33.0	9.0	**42.0**	33.0	11.5	**44.5**
	B4	68.235	33.0	9.0	**42.0**	33.0	11.5→14	-
	B5	68.235	33.0	9→11.5	-	33.0	14.0	**47.0**
	B6	100.530	33.0	11.5	**44.5**	33.0	14.0	**47.0**
M1	B1	98.530	33.0	11.5	**44.5**	33.0	14.0	**47.0**
	B2	96.530	33.0	11.5	**44.5**	33.0	14.0	**47.0**
	B4	96.530	33.0	11.5	**44.5**	33.0	14.0	**47.0**
	B5	98.530	33.0	11.5→9	-	33.0	14.0	**47.0**
P1	B1	100.530	33.0	9.0	**42.0**	33.0	14.0	**47.0**
	B2	68.235	33.0	9.0	**42.0**	33.0	14.0	**47.0**
	B3	68.235	33.0	9.0	**42.0**	33.0	14→9	-
	B4	101.380	33.0	9.0	**42.0**	33.0	9.0	**42.0**
	B5	100.420	33.0	9.0	**42.0**	33.0	9.0	**42.0**
	B6	101.200	33.0	9.0	**42.0**	33.0	9.0	**42.0**
P2	B1	54.310	33.0	9.0	**42.0**	33.0	9.0	**42.0**
	B2	53.310	33→15	9.0	-	33→15	9.0	-
	B3	80.430	15.0	9.0	**24.0**	15.0	9.0	**24.0**
	B4	91.950	15.0	9.0	**24.0**	15.0	9.0	**24.0**
P3	B1	104.470	15.0	3.7	**18.7**	15.0	3.7	**18.7**
	B2	97.110	12.0	0.0	**12.0**	12.0	0.0	**12.0**

Table D2. Results of Analysis

UDS TRAY PNI RESULTS

OPERATING ALTITUDE = 400 KM
SOLAR FLUX = 70x10**4 JY

ORBIT INCLINATION = 28.5
STARTING DATE = 1995

Avionics Area = 170.3 M^2
Fluids Area = 59.45 M^2

UDS EXPOSURE TIME = 10 YEARS

Test Dia in"	Energy Scaled Dia Met cm	Energy Scaled Dia Deb cm	Fluid section PNI% Met	Fluid section PNI% Deb	Fluid section # IMPACTS Nmet	Fluid section # IMPACTS Ndeb	Avionics section PNI% Met	Avionics section PNI% Deb	Avionics section # IMPACTS Nmet	Avionics section # IMPACTS Ndeb	Fluids-TOT PNI%	Fluids-TOT N	Avion.-TOT PNI%	Avion.-TOT N	N TOT	PNI% TOT
(1/64)	0.026	0.03	0	0	280.5	22.87	0	0	781	65	0	303.4	0	846	1149	0
(1/32)	0.053	0.06	0	1.754	26.51	4.043	0	0	74	11.58	0	30.55	0	85.58	116.1	0
(1/16)	0.106	0.119	11.89	48.16	2.13	0.731	0.234	12.33	6.056	2.093	5.724	2.86	0.029	8.149	11.01	0.002
(3/32)	0.159	0.179	63.04	76.78	0.461	0.264	26.86	46.91	1.314	0.757	48.4	0.726	12.6	2.071	2.797	6.1
(1/8)	0.267	0.238	94.1	87.77	0.063	0.13	83.8	68.82	0.175	0.374	82.59	0.194	57.67	0.548	0.742	47.63
(1/4)	0.533	0.476	99.58	97.59	0.004	0.024	98.82	93.24	0.012	0.07	97.18	0.029	92.14	0.082	0.11	89.54
(3/8)	0.8	0.715	99.92	99.03	8E-04	0.01	99.76	97.24	0.002	0.028	98.94	0.011	97.01	0.03	0.041	95.98

UDS EXPOSURE TIME = 30 YEARS

Test Dia in"	Energy Scaled Dia Met cm	Energy Scaled Dia Deb cm	Fluid section PNI% Met	Fluid section PNI% Deb	Fluid section # IMPACTS Nmet	Fluid section # IMPACTS Ndeb	Avionics section PNI% Met	Avionics section PNI% Deb	Avionics section # IMPACTS Nmet	Avionics section # IMPACTS Ndeb	Fluids-tot PNI%	Fluids-tot N	Avion.-tot PNI%	Avion.-tot N	N TOT	PNI% TOT
(1/64)	0.026	0.03	0	0	832	92	0	0	2393	260	0	1092	0	2485	3577	0
(1/32)	0.053	0.06	0	0	79	16.34	0	0	224	47	0	126	0	240.3	366.3	0
(1/16)	0.106	0.119	0.019	5.221	6.35	2.952	1E-06	0.021	18.65	8.457	1E-03	14.81	3E-10	21.6	36.41	3E-15
(3/32)	0.159	0.179	25.05	34.38	1.384	1.067	1.939	4.698	3.943	3.058	8.613	4.442	0.091	5.01	9.452	0.008
(1/8)	0.267	0.238	82.05	59.04	0.186	0.527	58.51	22.1	0.532	1.51	48.44	1.696	12.93	1.059	2.755	6.264
(1/4)	0.533	0.476	98.76	90.6	0.013	0.099	96.5	75.38	0.036	0.283	89.48	0.295	72.74	0.134	0.429	65.08
(3/8)	0.8	0.715	99.75	96.13	0.003	0.039	99.29	89.32	0.007	0.113	95.89	0.115	88.68	0.047	0.162	85.03

REPORT DOCUMENTATION PAGE

Form Approved
OMB No. 0704-0188

1. AGENCY USE ONLY *(Leave blank)*

2. REPORT DATE
July 1993

3. REPORT TYPE AND DATES COVERED
Technical Memorandum

4. TITLE AND SUBTITLE
Hypervelocity Impact Testing of the Space Station Utility Distribution System Carrier

5. FUNDING NUMBERS

6. AUTHOR(S)

Scott Lazaroff, Johnson Space Center

7. PERFORMING ORGANIZATION NAME(S) AND ADDRESS(ES)

Propulsion and Power Division
Lyndon B. Johnson Space Center
Houston, Texas 77058

8. PERFORMING ORGANIZATION REPORT NUMBER

S-723

9. SPONSORING / MONITORING AGENCY NAME(S) AND ADDRESS(ES)

National Aeronautics and Space Administration
Washington, D.C. 20546

10. SPONSORING / MONITORING AGENCY REPORT NUMBER

NASA-TM-104771

11. SUPPLEMENTARY NOTES

12a. DISTRIBUTION / AVAILABILITY STATEMENT
National Technical Information Service
5285 Port Royal Road
Springfield, VA 22161
(703) 487-4600
Unclassified/Unlimited Subject Category 20

12b. DISTRIBUTION CODE

13. ABSTRACT *(Maximum 200 words)*

A two-phase joint NASA Johnson Space Center and McDonnell Douglas Aerospace-Huntington Beach hypervelocity impact (HVI) test program was initiated to develop an improved understanding of how meteoroid and orbital debris (M/OD) impacts affect the Space Station Freedom (SSF) avionic and fluid lines routed in the Utility Distribution System (UDS) carrier. This report documents the first phase of the test program which covers nonpowered avionic line segment and pressurized fluid line segment HVI testing. From these tests, a better estimation of avionic line failures is approximately 15 failures per year and could very well drop to around 1 or 2 avionic line failures per year (depending upon the results of the second phase testing of the powered avionic line at White Sands). For the fluid lines, the initial McDonnell Douglas analysis calculated 1 to 2 line failures over a 30 year period. The data obtained from these tests indicate the number of predicted fluid line failures increased slightly to as many as 3 in the first 10 years and up to 15 for the entire 30 year life of SSF.

14. SUBJECT TERMS
Hypervelocity Impact, Meteoritic Damage, Space Debris (Damage), Impact Damage, Impact Tests,

15. NUMBER OF PAGES
60

16. PRICE CODE

17. SECURITY CLASSIFICATION OF REPORT
Unclassified

18. SECURITY CLASSIFICATION OF THIS PAGE
Unclassified

19. SECURITY CLASSIFICATION OF ABSTRACT
Unclassified

20. LIMITATION OF ABSTRACT
Unlimited